Detecting chaos in Hamiltonian systems by the Smaller (SALI) and the Generalized (GALI) Alignment Index methods

Haris Skokos

Department of Mathematics and Applied Mathematics
University of Cape Town
Cape Town, South Africa

E-mail: haris.skokos@uct.ac.za
URL: http://math_research.uct.ac.za/~hskokos/

National Technical University of Athens, Greece, 23 May 2022

Outline

- Dynamical Systems
  - ✓ Hamiltonian models – Variational equations
  - ✓ Symplectic maps – Tangent map

- Chaos Indicators
  - ✓ Maximum Lyapunov Exponent
  - ✓ Smaller ALignment Index – SALI
    - Definition
    - Behavior for chaotic and regular motion
    - Applications
  - ✓ Generalized ALignment Index – GALI
    - Definition - Relation to SALI
    - Behavior for chaotic and regular motion
    - <u>Application to time-dependent models</u>

Autonomous Hamiltonian systems

Consider an N degree of freedom autonomous Hamiltonian system having a Hamiltonian function of the form:

$$H(\underbrace{q_1,q_2,\ldots,q_N}_{\text{positions}},\ \underbrace{p_1,p_2,\ldots,p_N}_{\text{momenta}})$$

The time evolution of an orbit (trajectory) with initial condition

$$P(0)=(q_1(0),\ q_2(0),\ldots,q_N(0),\ p_1(0),\ p_2(0),\ldots,p_N(0))$$

is governed by the Hamilton's equations of motion

$$\frac{dp_i}{dt} = -\frac{\partial H}{\partial q_i}\ ,\qquad \frac{dq_i}{dt} = \frac{\partial H}{\partial p_i}$$

Variational Equations

We use the notation $\mathbf{x} = (q_1,q_2,\ldots,q_N,p_1,p_2,\ldots,p_N)^T$. The deviation vector from a given orbit is denoted by

$$\mathbf{v} = (\delta x_1, \delta x_2,\ldots,\delta x_n)^T \text{, with } n=2N$$

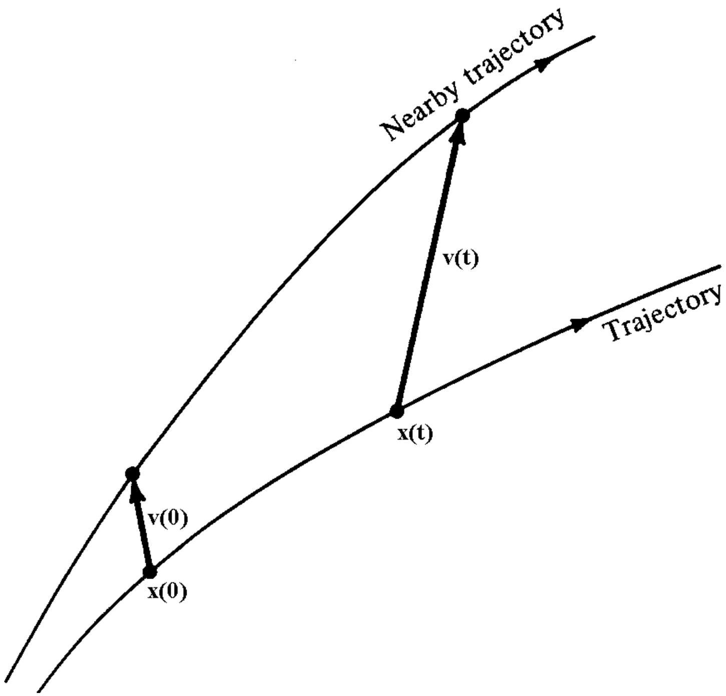

Benettin & Galgani, 1979, in Laval and Gressillon (eds.), op cit, 93

The time evolution of v is given by the so-called variational equations:

$$\frac{d\mathbf{v}}{dt} = -\mathbf{J} \cdot \mathbf{P} \cdot \mathbf{v}$$

where

$$\mathbf{J} = \begin{pmatrix} 0_N & -I_N \\ I_N & 0_N \end{pmatrix}, \quad P_{ij} = \frac{\partial^2 H}{\partial x_i \partial x_j} \quad i,j = 1,2,\ldots,n$$

Symplectic Maps

Consider an 2N-dimensional symplectic map T. In this case we have discrete time.

The evolution of an orbit with initial condition

$$P(0)=(x_1(0), x_2(0),\ldots,x_{2N}(0))$$

is governed by the equations of map T

$$P(i+1)=T\,P(i)\ ,\ i=0,1,2,\ldots$$

The evolution of an initial deviation vector

$$v(0) = (\delta x_1(0), \delta x_2(0),\ldots, \delta x_{2N}(0))$$

is given by the corresponding tangent map

$$v(i+1) = \left.\frac{\partial T}{\partial P}\right|_i \cdot v(i)\ ,\ i = 0,1,2,\ldots$$

Maximum Lyapunov Exponent

Roughly speaking, the Lyapunov exponents of a given orbit characterize the mean exponential rate of divergence of trajectories surrounding it.

Consider an orbit in the 2N-dimensional phase space with initial condition x(0) and an initial deviation vector from it v(0). Then the mean exponential rate of divergence is:

$$\mathrm{mLCE} = \sigma_1 = \lim_{t \to \infty} \frac{1}{t} \ln \frac{\|\vec{v}(t)\|}{\|\vec{v}(0)\|}$$

$\sigma_1 = 0 \rightarrow$ Regular motion

$\sigma_1 \neq 0 \rightarrow$ Chaotic motion

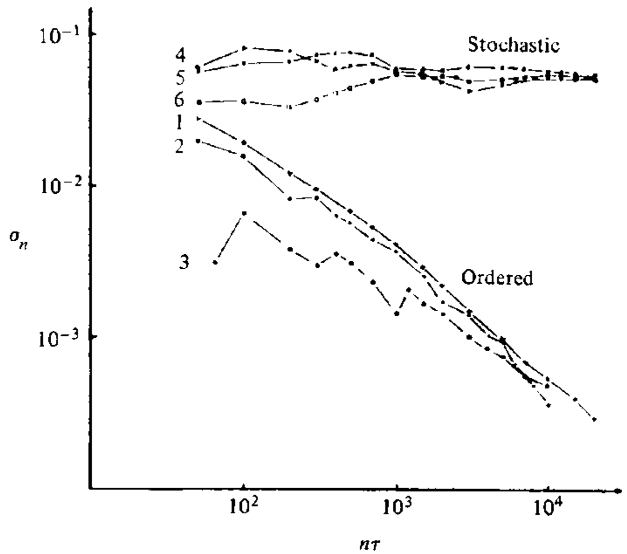

Figure 5.7. Behavior of σ_n at the intermediate energy $E = 0.125$ for initial points taken in the ordered (curves 1–3) or stochastic (curves 4–6) regions (after Benettin *et al.*, 1976).

If we start with more than one linearly independent deviation vectors they will align to the direction defined by the largest Lyapunov exponent for chaotic orbits.

The
Smaller ALignment Index
(SALI)
method

Definition of the SALI

We follow the evolution in time of <u>two different initial deviation vectors</u> ($v_1(0)$, $v_2(0)$), and define the SALI (Ch.S. 2001, J. Phys. A) as:

$$SALI(t) = \min\left\{ \left\| \hat{v}_1(t) + \hat{v}_2(t) \right\|, \left\| \hat{v}_1(t) - \hat{v}_2(t) \right\| \right\}$$

where

$$\hat{v}_1(t) = \frac{v_1(t)}{\left\| v_1(t) \right\|}$$

When the two vectors become collinear

$$SALI(t) \rightarrow 0$$

Behavior of the SALI for chaotic motion

For chaotic orbits the two initially different deviation vectors tend to coincide with the direction defined by the maximum Lyapunov exponent.

Behavior of the SALI for chaotic motion

For chaotic orbits the two initially different deviation vectors tend to coincide with the direction defined by the maximum Lyapunov exponent.

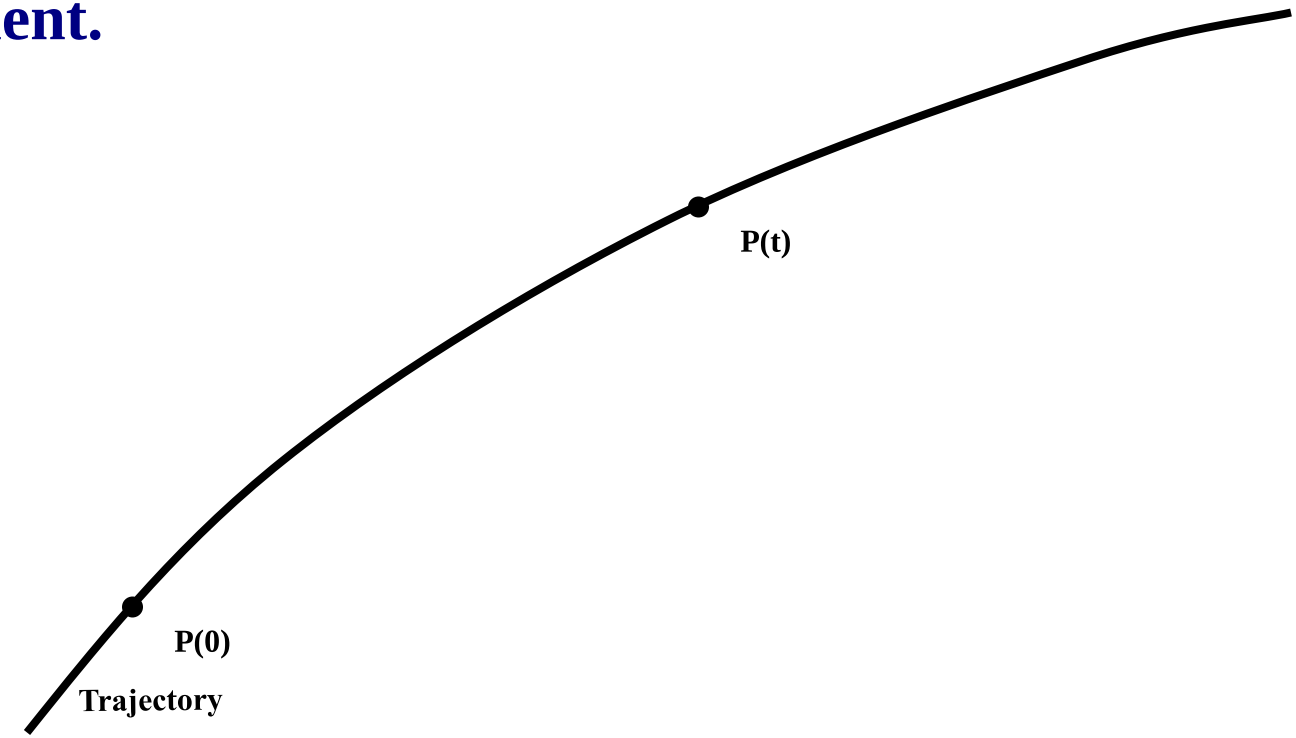

Behavior of the SALI for chaotic motion

For chaotic orbits the two initially different deviation vectors tend to coincide with the direction defined by the maximum Lyapunov exponent.

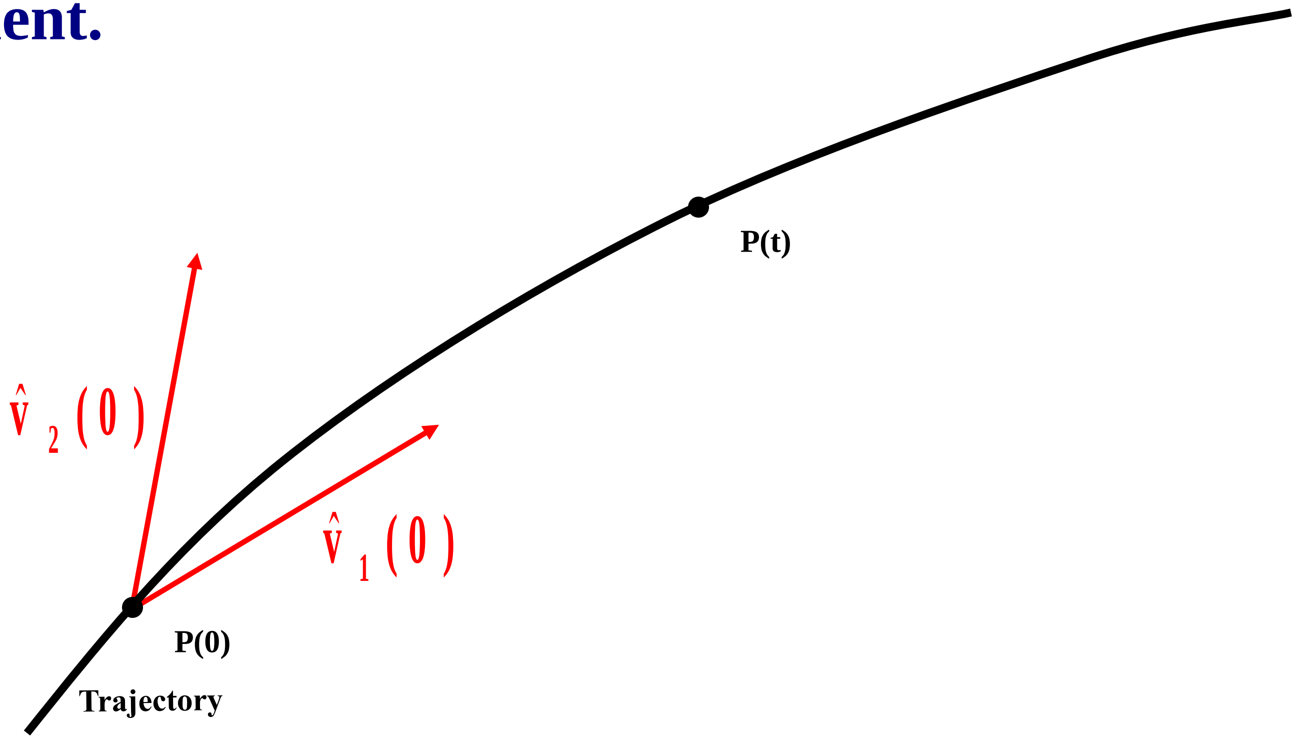

Behavior of the SALI for chaotic motion

For chaotic orbits the two initially different deviation vectors tend to coincide with the direction defined by the maximum Lyapunov exponent.

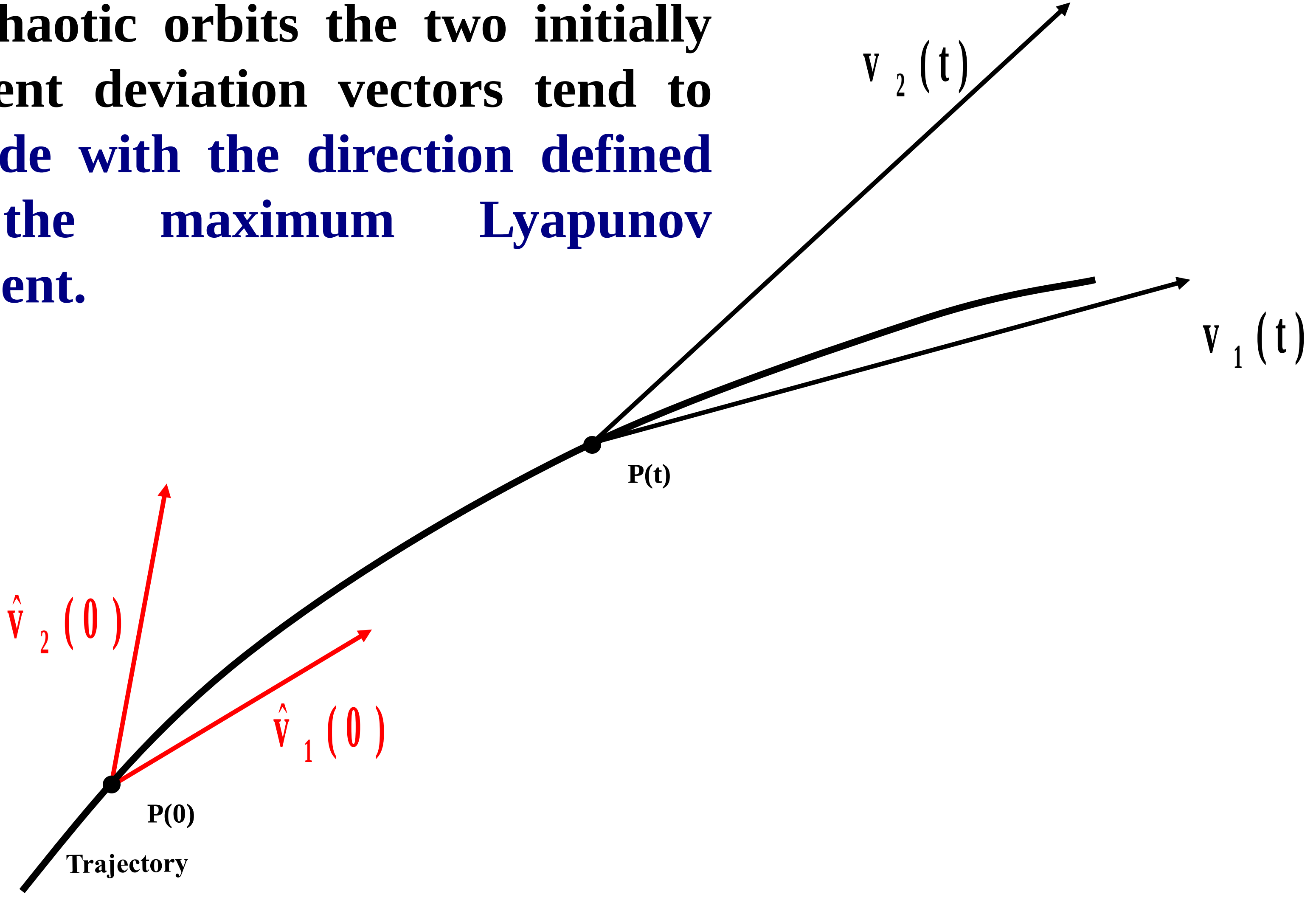

Behavior of the SALI for chaotic motion

For chaotic orbits the two initially different deviation vectors tend to coincide with the direction defined by the maximum Lyapunov exponent.

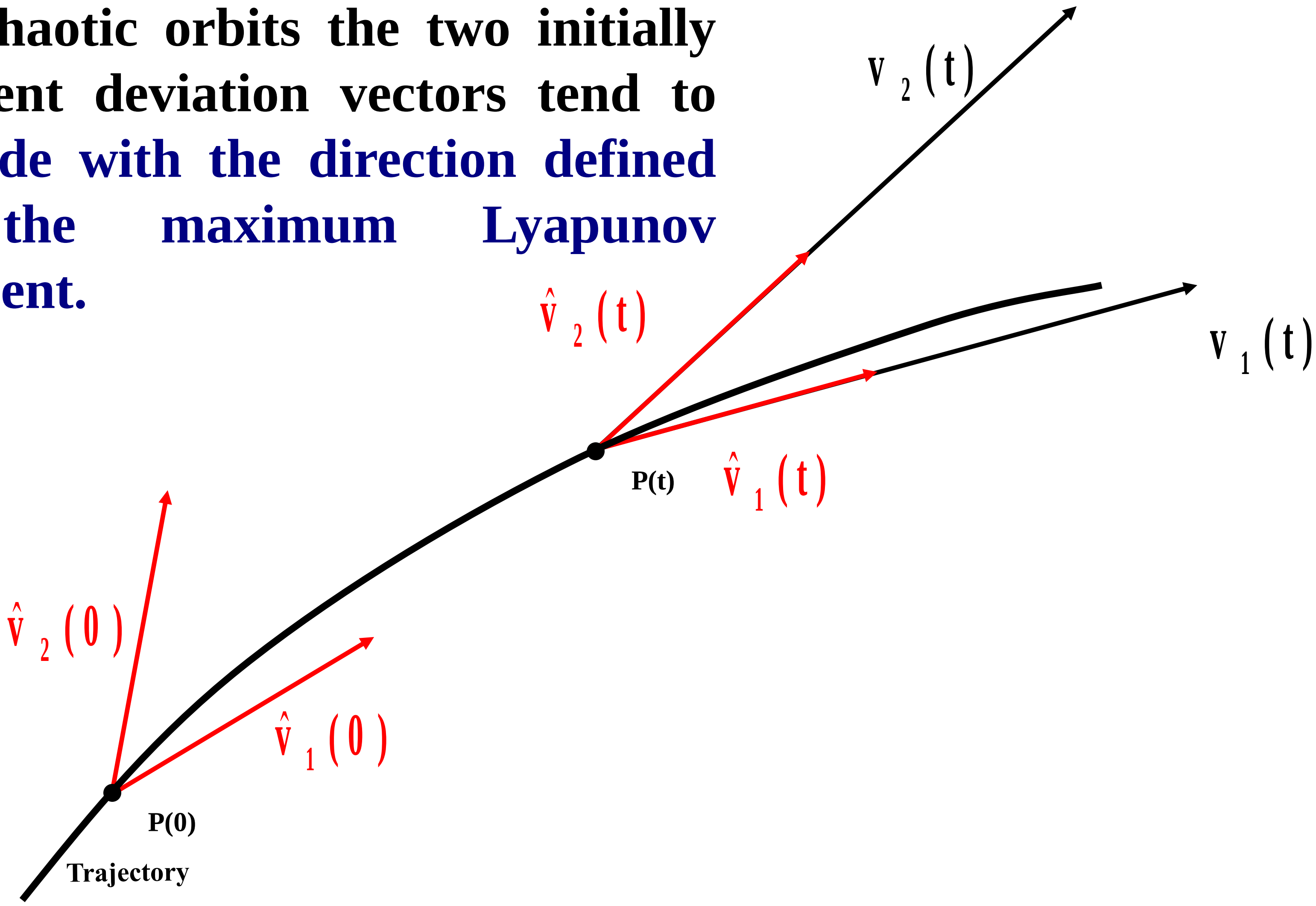

Behavior of the SALI for chaotic motion

For chaotic orbits the two initially different deviation vectors tend to coincide with the direction defined by the maximum Lyapunov exponent.

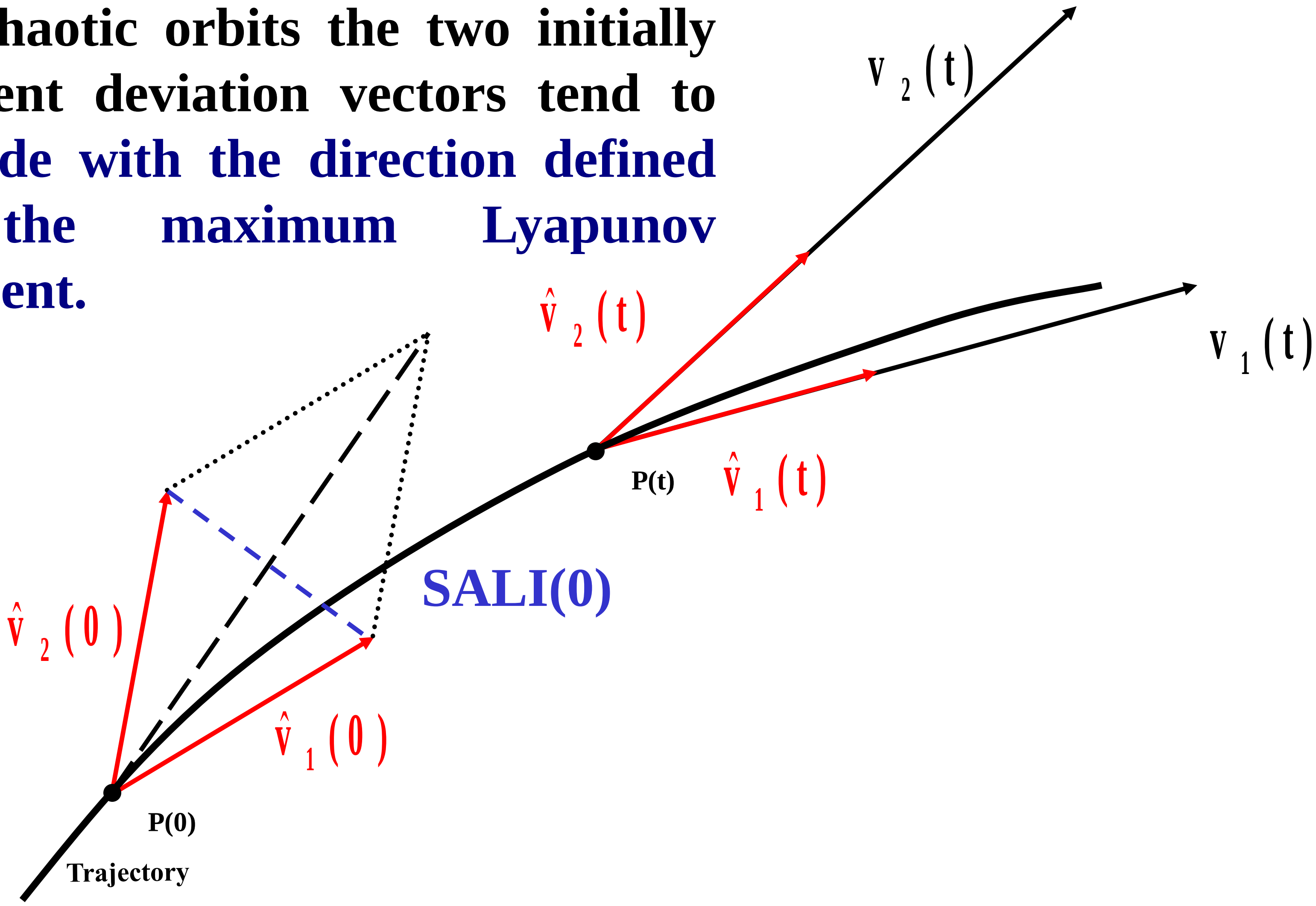

Behavior of the SALI for chaotic motion

For chaotic orbits the two initially different deviation vectors tend to coincide with the direction defined by the maximum Lyapunov exponent.

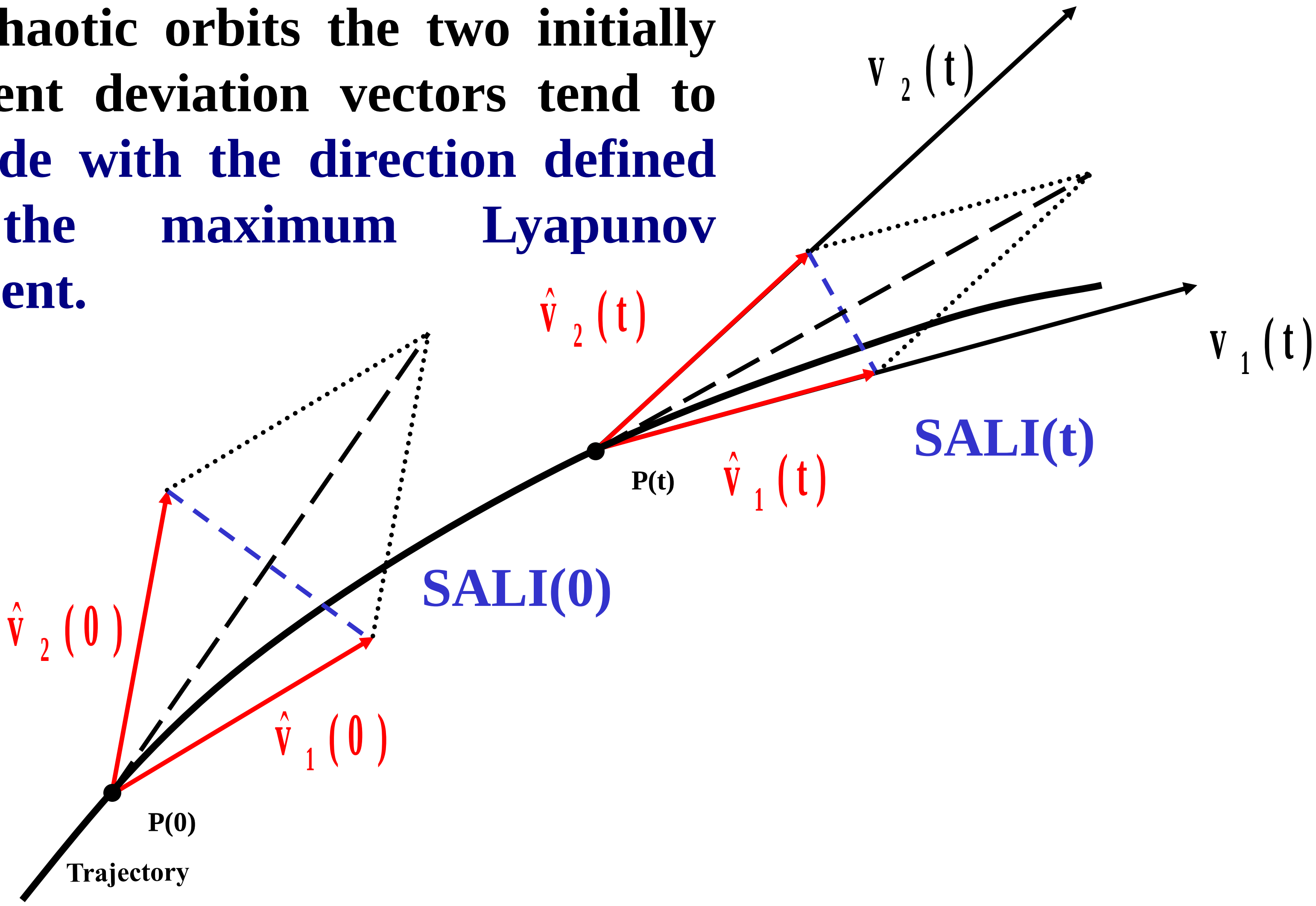

Behavior of the SALI for chaotic motion

We test the validity of the approximation $SALI \propto e^{-(\sigma_1-\sigma_2)t}$ (Ch.S., Antonopoulos, Bountis, Vrahatis, 2004, J. Phys. A) for a chaotic orbit of the 3D Hamiltonian

$$H = \sum_{i=1}^{3} \frac{\omega_i}{2}(q_i^2 + p_i^2) + q_1^2 q_2 + q_1^2 q_3$$

with ω_1=1, ω_2=1.4142, ω_3=1.7321, H=0.09

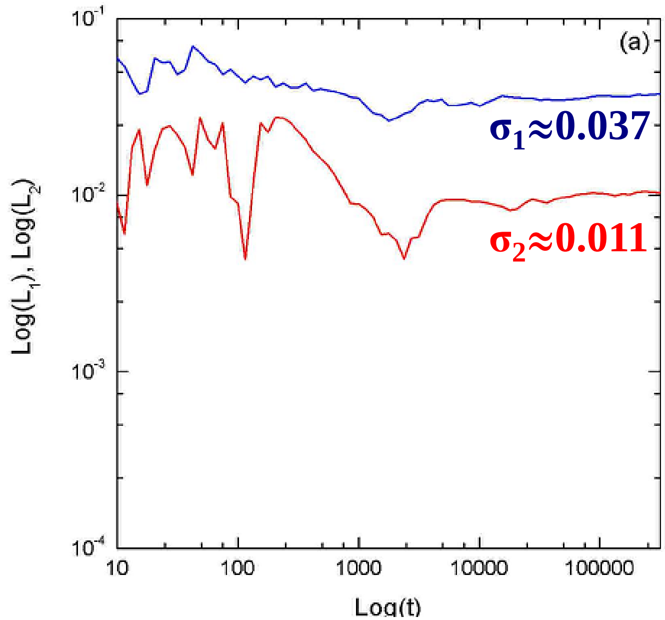

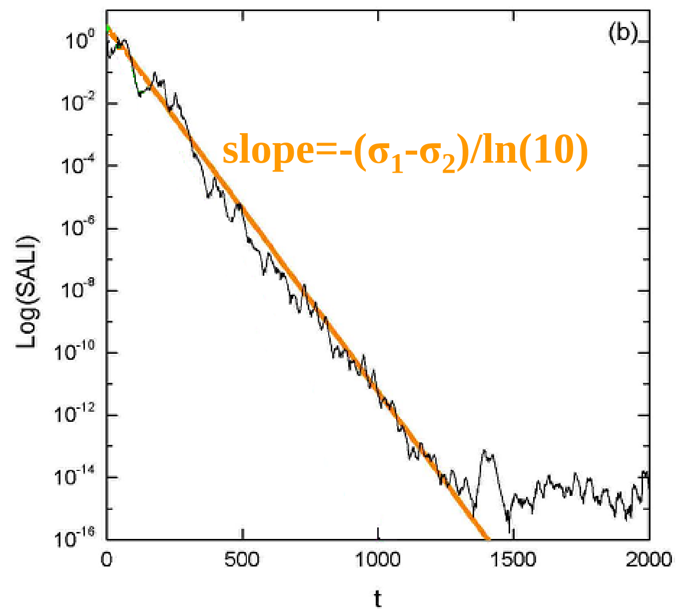

Behavior of the SALI for regular motion

Regular motion occurs on a torus and two different initial deviation vectors become tangent to the torus, generally having different directions.

Behavior of the SALI for regular motion

Regular motion occurs on a torus and two different initial deviation vectors become tangent to the torus, generally having different directions.

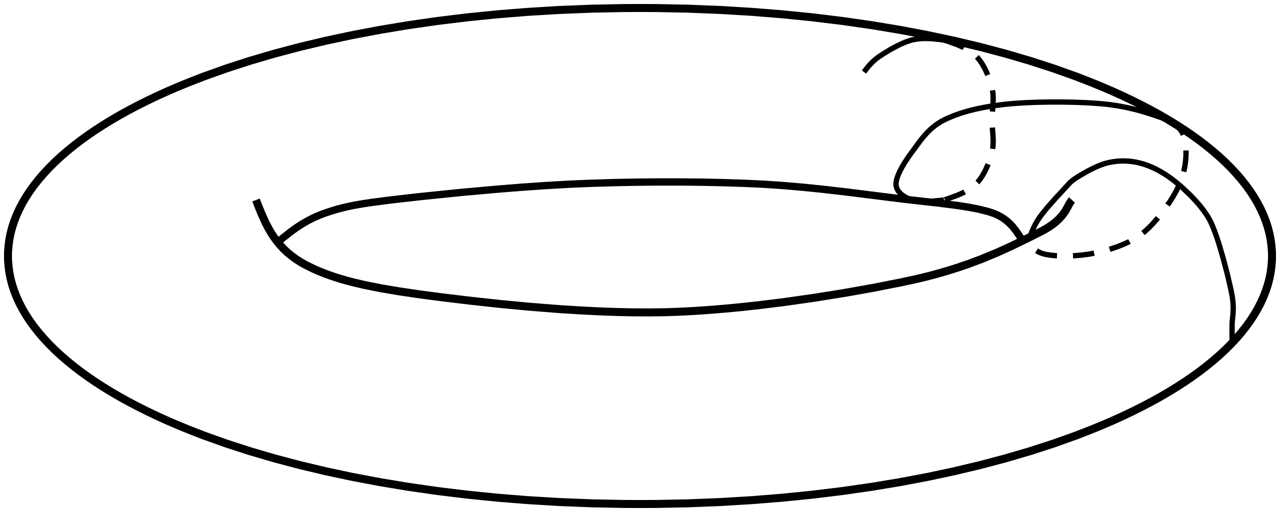

Behavior of the SALI for regular motion

Regular motion occurs on a torus and two different initial deviation vectors become tangent to the torus, generally having different directions.

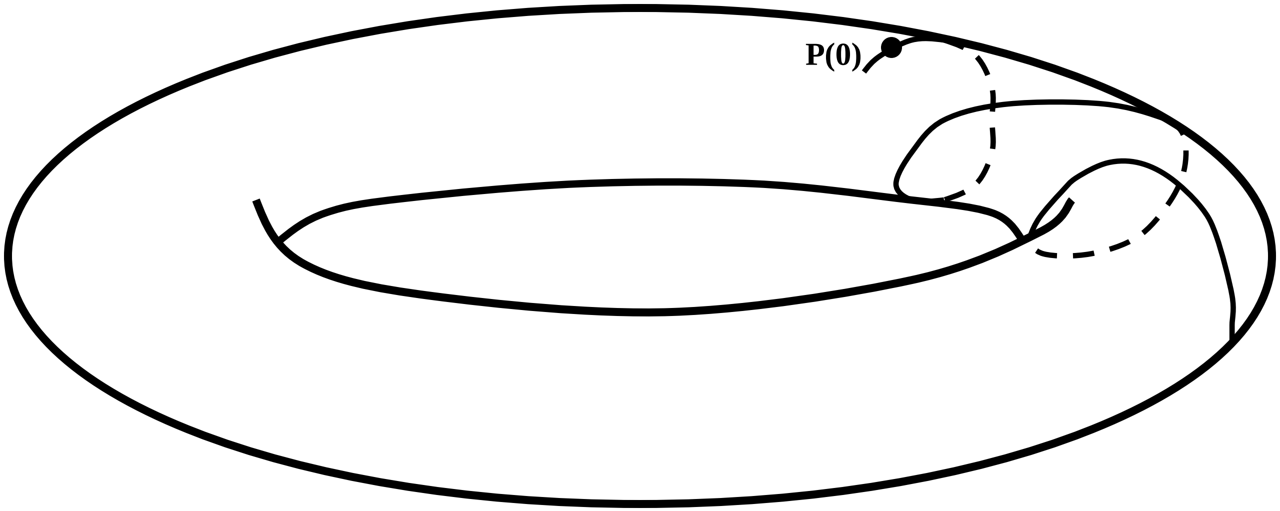

Behavior of the SALI for regular motion

Regular motion occurs on a torus and two different initial deviation vectors become tangent to the torus, generally having different directions.

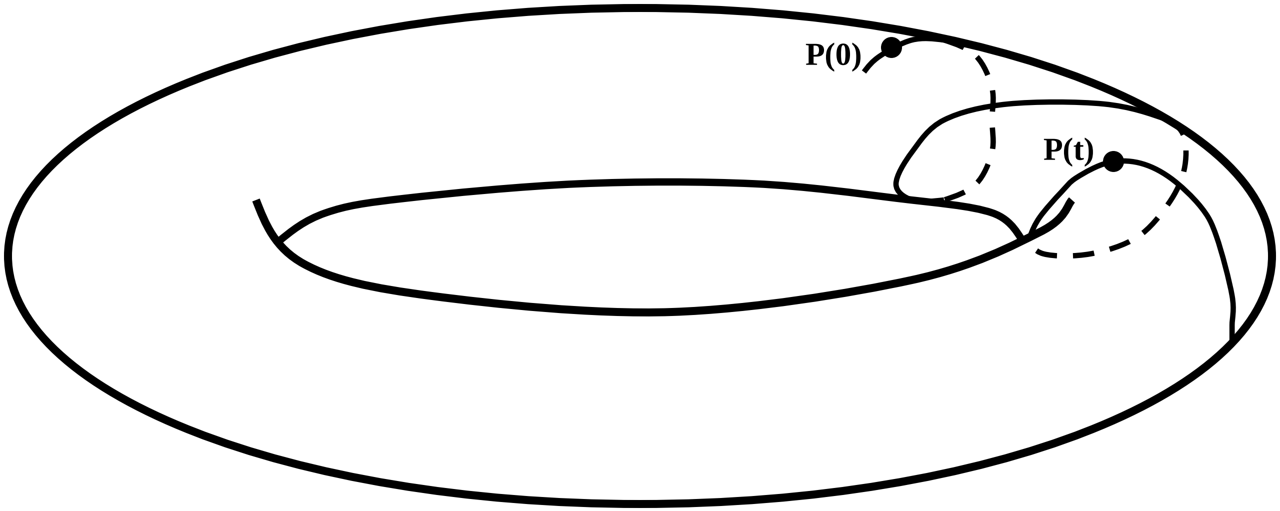

Behavior of the SALI for regular motion

Regular motion occurs on a torus and two different initial deviation vectors become tangent to the torus, generally having different directions.

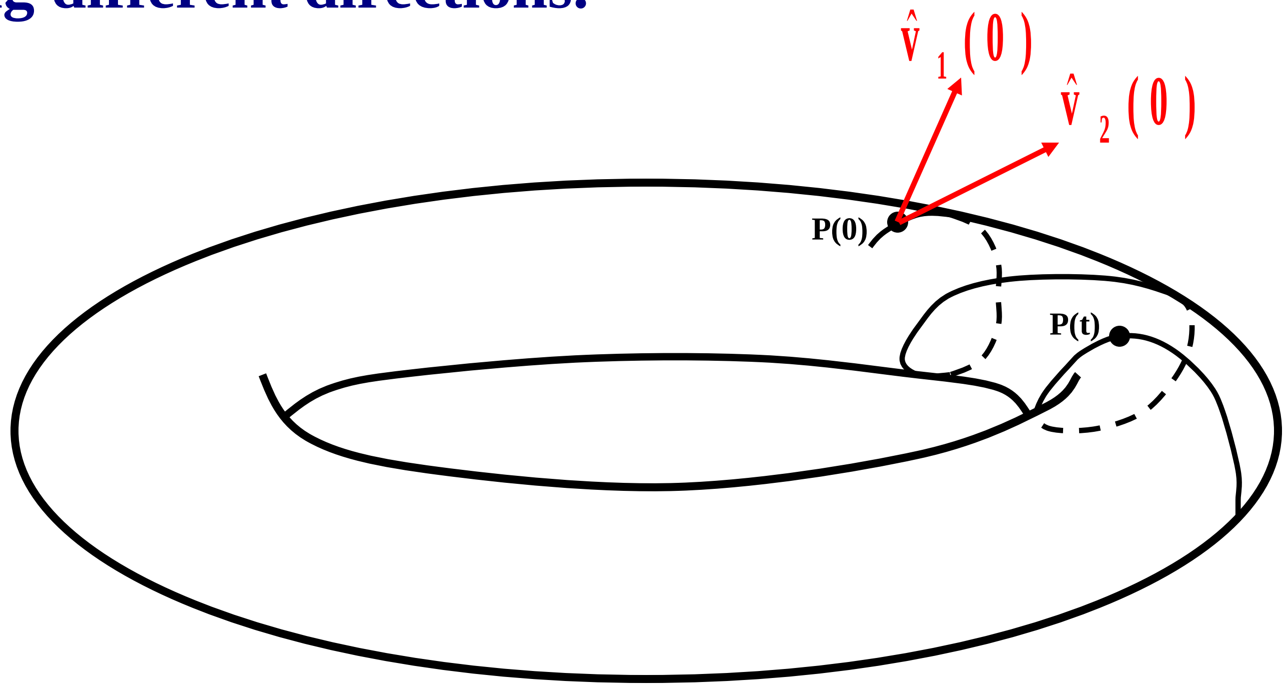

Behavior of the SALI for regular motion

Regular motion occurs on a torus and two different initial deviation vectors become tangent to the torus, generally having different directions.

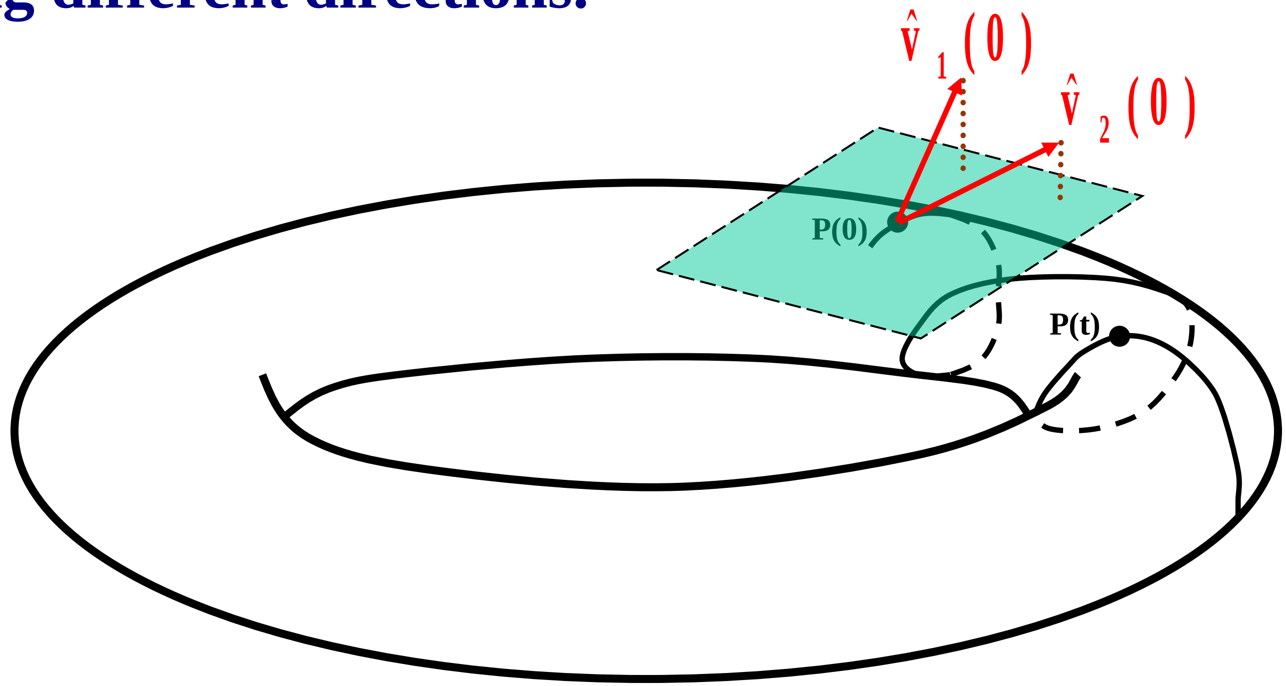

Behavior of the SALI for regular motion

Regular motion occurs on a torus and two different initial deviation vectors become tangent to the torus, generally having different directions.

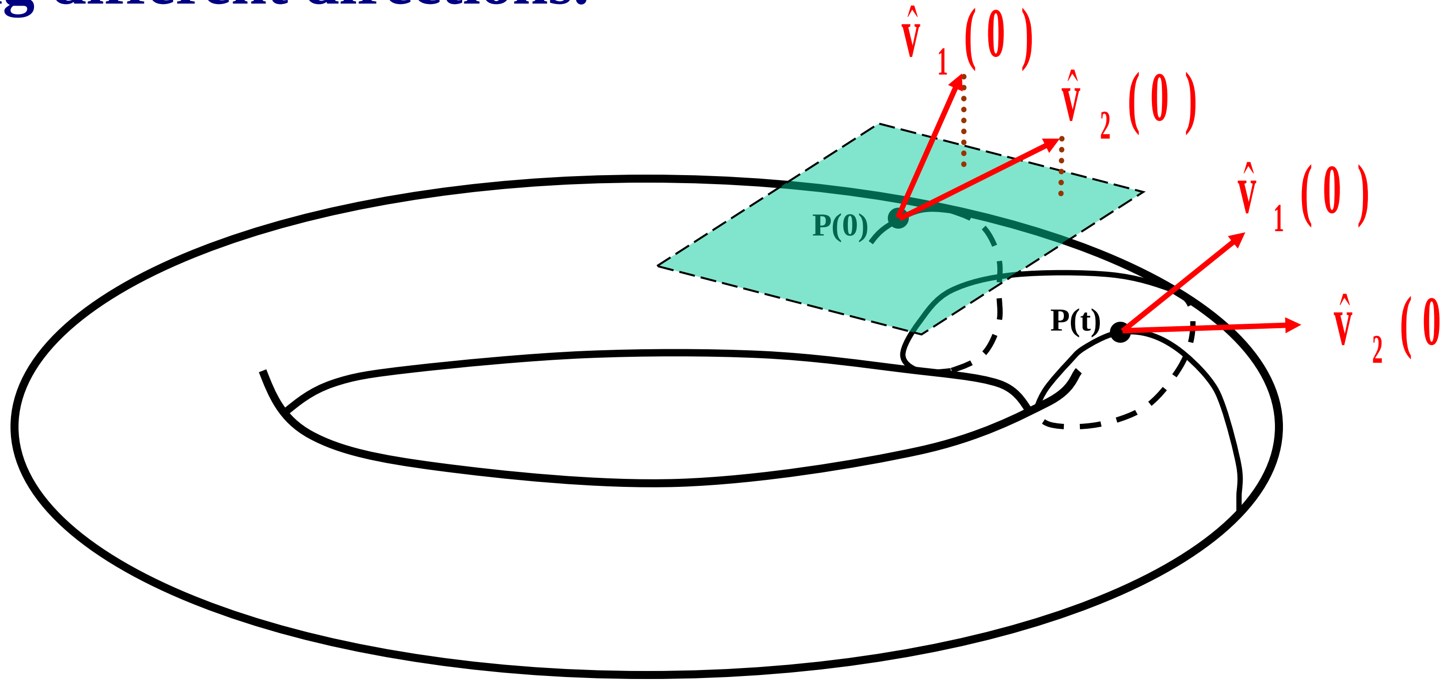

Behavior of the SALI for regular motion

Regular motion occurs on a torus and two different initial deviation vectors become tangent to the torus, generally having different directions.

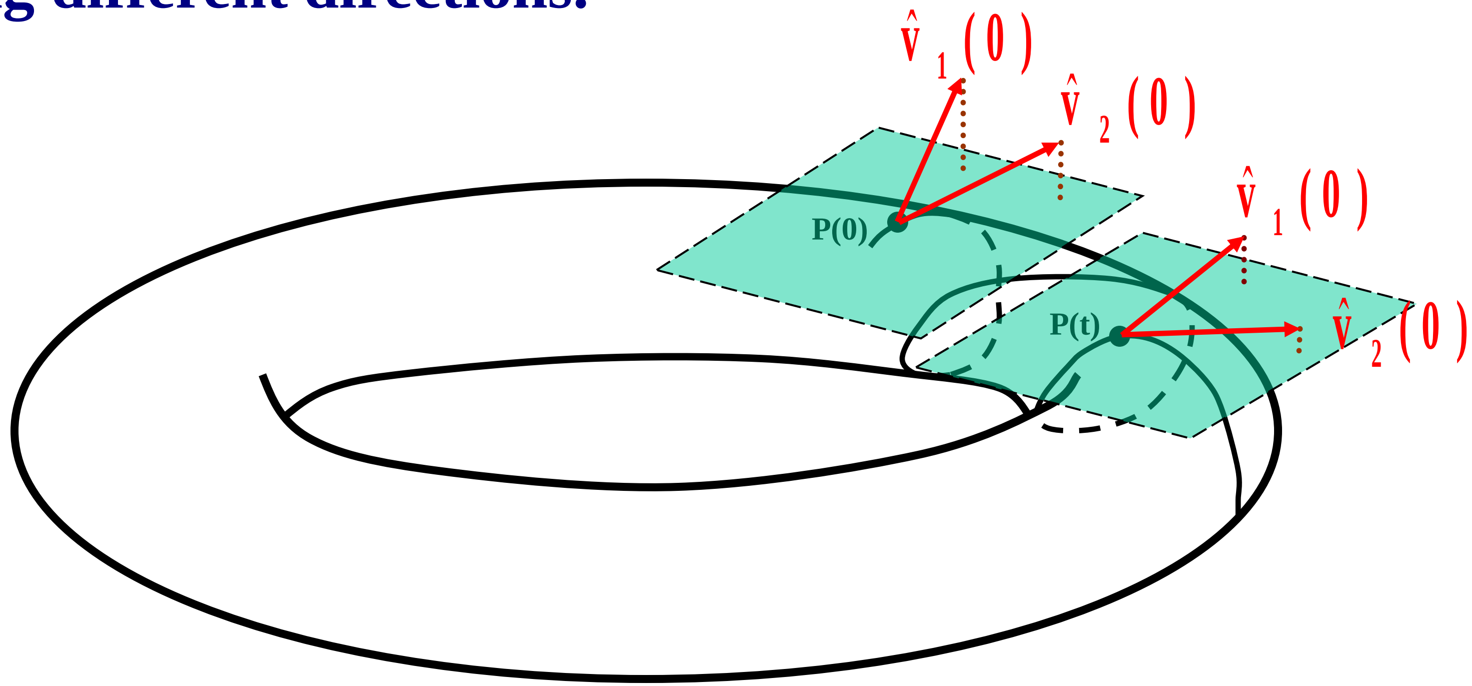

Applications – Hénon-Heiles system

As an example, we consider the 2D Hénon-Heiles system:

$$H_2 = \frac{1}{2}(p_x^2 + p_y^2) + \frac{1}{2}(x^2 + y^2) + x^2 y - \frac{1}{3}y^3$$

For E=1/8 we consider the orbits with initial conditions:
Regular orbit, x=0, y=0.55, p_x=0.2417, p_y=0
Chaotic orbit, x=0, y=-0.016, p_x=0.49974, p_y=0
Chaotic orbit, x=0, y=-0.01344, p_x=0.49982, p_y=0

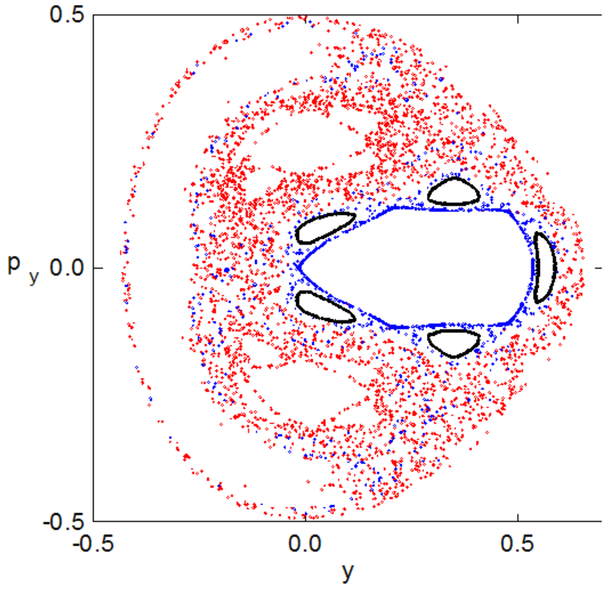

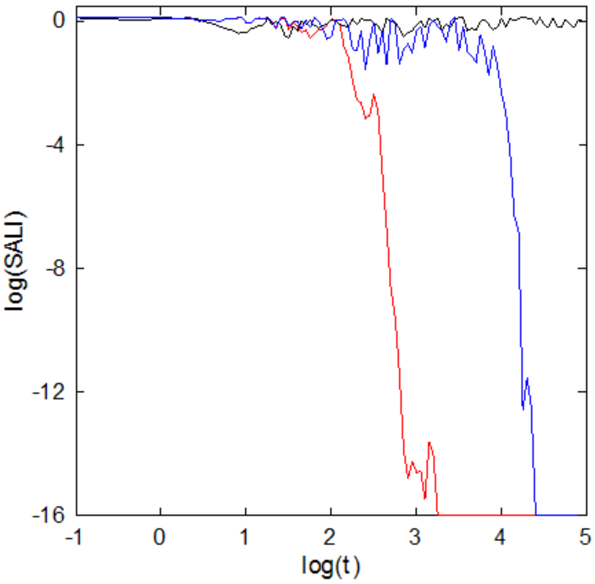

Applications – Hénon-Heiles system

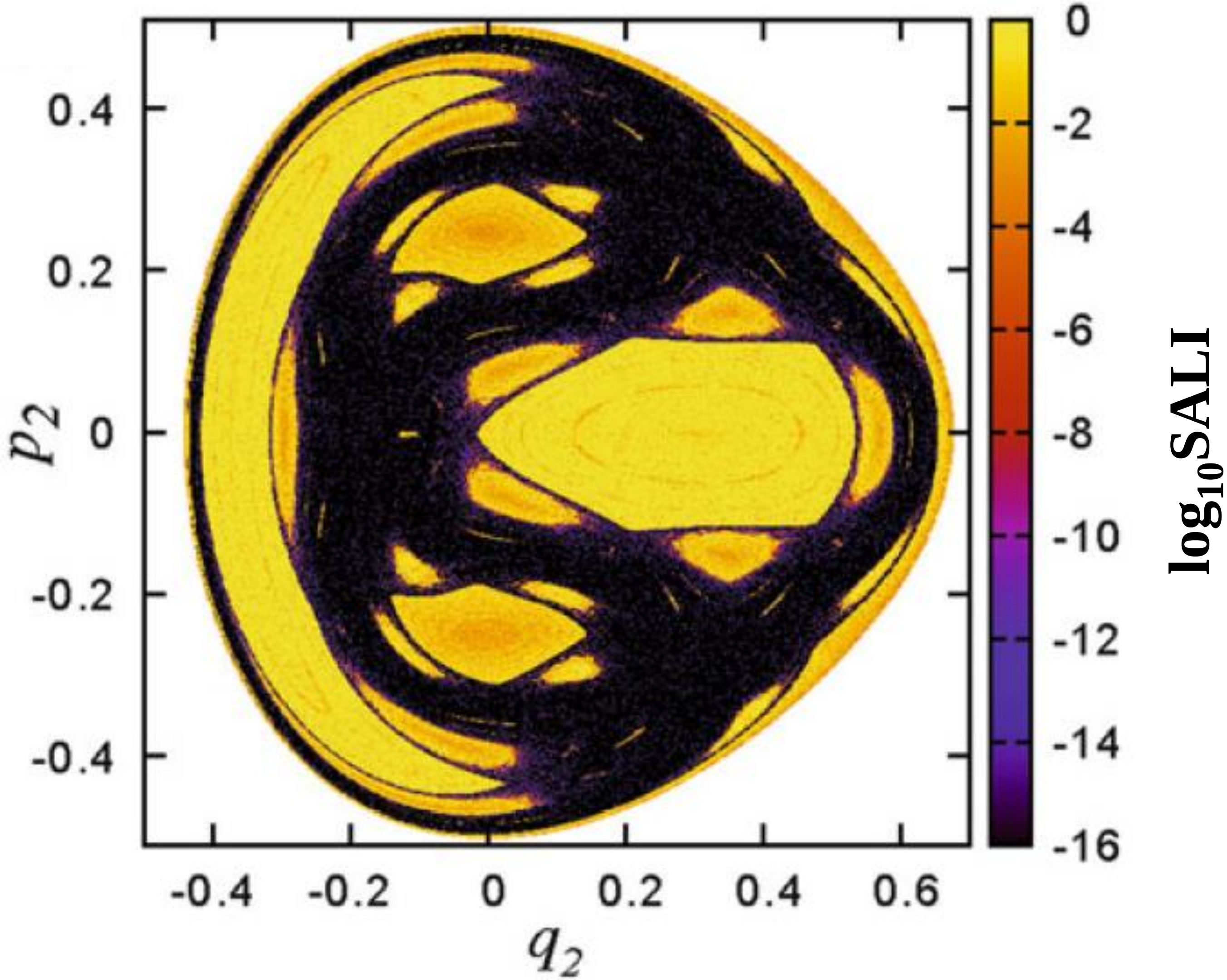

Applications – 4D map

$$
\begin{aligned}
x_1' &= x_1 + x_2 \\
x_2' &= x_2 - \nu \sin(x_1 + x_2) - \mu [1 - \cos(x_1 + x_2 + x_3 + x_4)] \\
x_3' &= x_3 + x_4 \\
x_4' &= x_4 - \kappa \sin(x_3 + x_4) - \mu [1 - \cos(x_1 + x_2 + x_3 + x_4)]
\end{aligned}
\quad (\text{mod } 2\pi)
$$

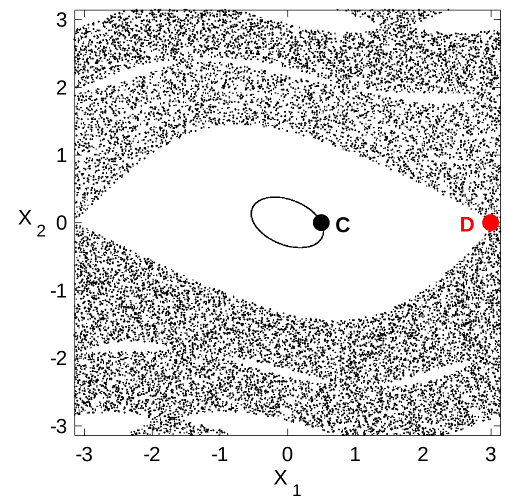

For ν=0.5, κ=0.1, μ=0.1 we consider the orbits:

***regular orbit C** with initial conditions $x_1=0.5$, $x_2=0$, $x_3=0.5$, $x_4=0$.*

***chaotic orbit D** with initial conditions $x_1=3$, $x_2=0$, $x_3=0.5$, $x_4=0$.*

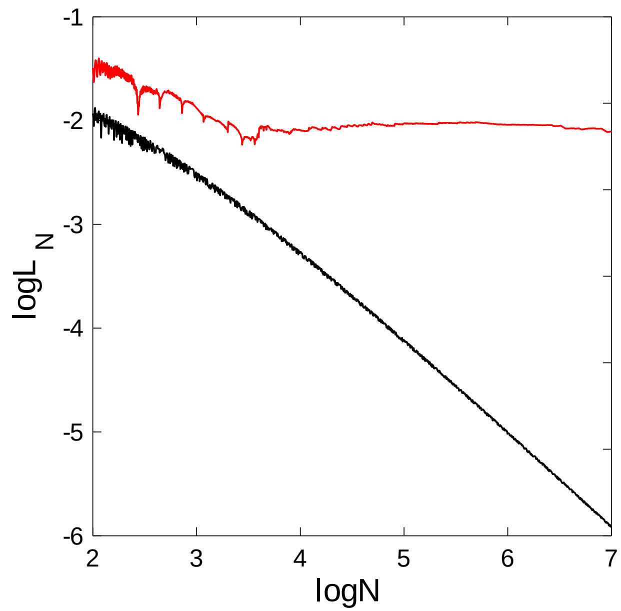

Applications – 4D map

$$\begin{aligned} x_1' &= x_1 + x_2 \\ x_2' &= x_2 - \nu \sin(x_1 + x_2) - \mu[1 - \cos(x_1 + x_2 + x_3 + x_4)] \\ x_3' &= x_3 + x_4 \\ x_4' &= x_4 - \kappa \sin(x_3 + x_4) - \mu[1 - \cos(x_1 + x_2 + x_3 + x_4)] \end{aligned} \quad (\mathrm{mod}\ 2\pi)$$

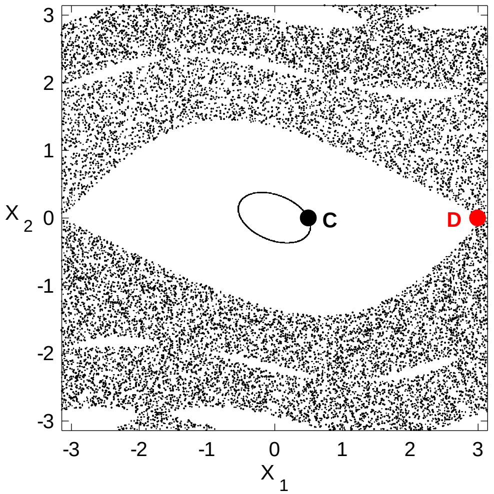

For ν=0.5, κ=0.1, μ=0.1 we consider the orbits:

***regular orbit C** with initial conditions x_1=0.5, x_2=0, x_3=0.5, x_4=0.*

***chaotic orbit D** with initial conditions x_1=3, x_2=0, x_3=0.5, x_4=0.*

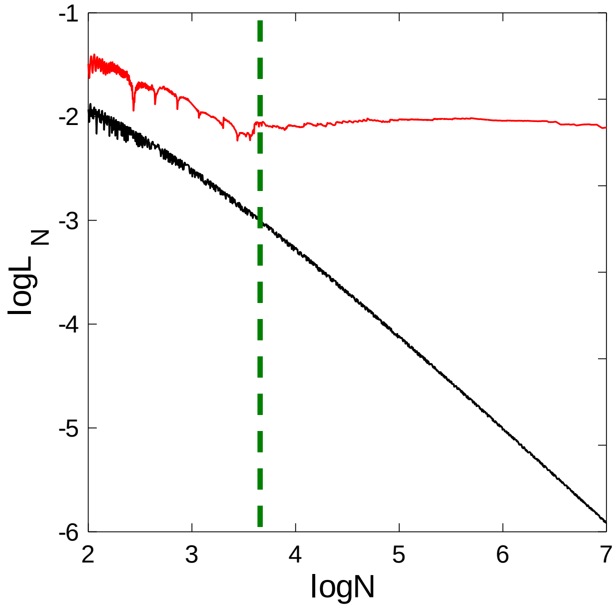

Applications – 4D map

$$\begin{aligned} x_1' &= x_1 + x_2 \\ x_2' &= x_2 - \nu \sin(x_1 + x_2) - \mu[1 - \cos(x_1 + x_2 + x_3 + x_4)] \\ x_3' &= x_3 + x_4 \\ x_4' &= x_4 - \kappa \sin(x_3 + x_4) - \mu[1 - \cos(x_1 + x_2 + x_3 + x_4)] \end{aligned} \quad (\text{mod } 2\pi)$$

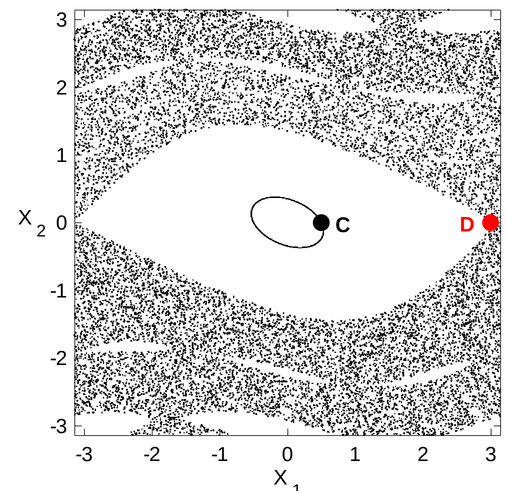

For ν=0.5, κ=0.1, μ=0.1 we consider the orbits:

regular orbit C *with initial conditions* $x_1=0.5$, $x_2=0$, $x_3=0.5$, $x_4=0$.

chaotic orbit D *with initial conditions* $x_1=3$, $x_2=0$, $x_3=0.5$, $x_4=0$.

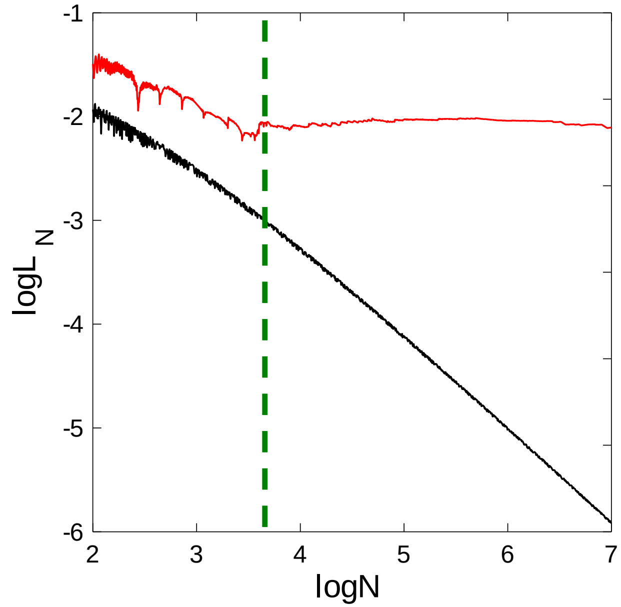

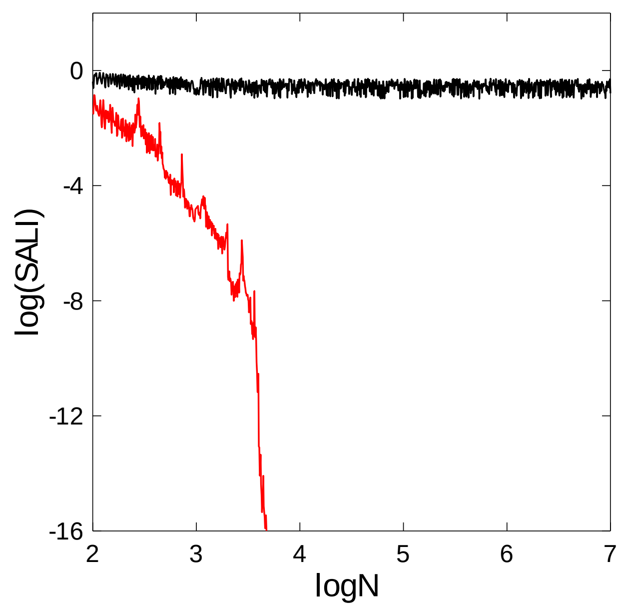

Applications – 4D map

$$
\begin{aligned}
x_1' &= x_1 + x_2 \\
x_2' &= x_2 - \nu \sin(x_1 + x_2) - \mu [1 - \cos(x_1 + x_2 + x_3 + x_4)] \\
x_3' &= x_3 + x_4 \\
x_4' &= x_4 - \kappa \sin(x_3 + x_4) - \mu [1 - \cos(x_1 + x_2 + x_3 + x_4)]
\end{aligned}
\quad (\text{mod } 2\pi)
$$

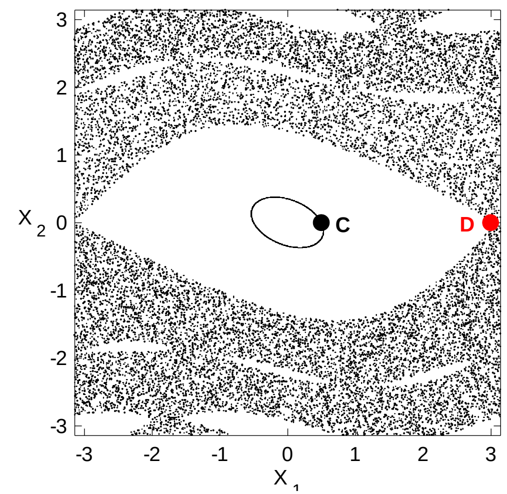

For ν=0.5, κ=0.1, μ=0.1 we consider the orbits:

***regular orbit C** with initial conditions x_1=0.5, x_2=0, x_3=0.5, x_4=0.*

***chaotic orbit D** with initial conditions x_1=3, x_2=0, x_3=0.5, x_4=0.*

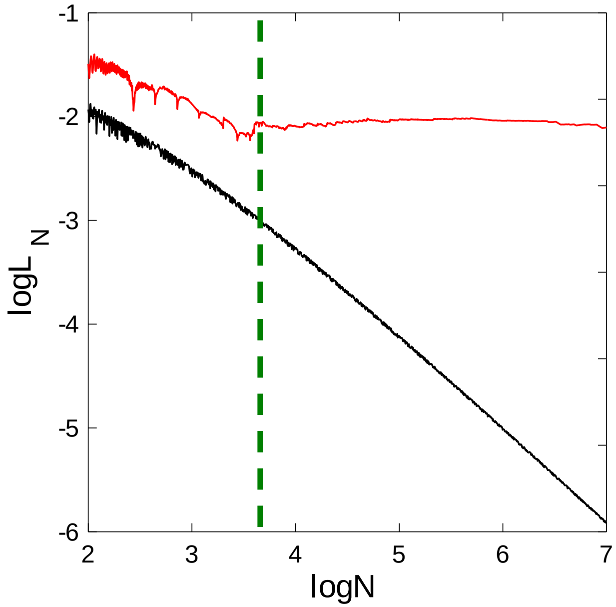

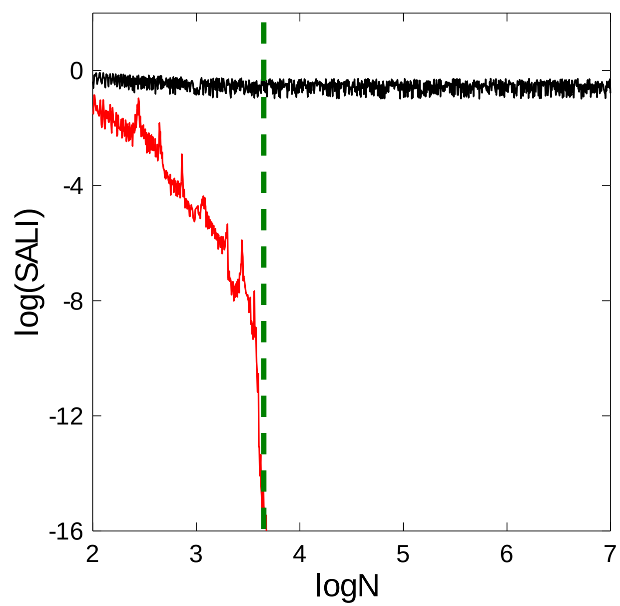

The
Generalized ALignment Indices
(GALIs)
method

Definition of the Generalized Alignment Index (GALI)

SALI effectively measures the 'area' of the parallelogram formed by the two deviation vectors.

Definition of the Generalized Alignment Index (GALI)

SALI effectively measures the 'area' of the parallelogram formed by the two deviation vectors.

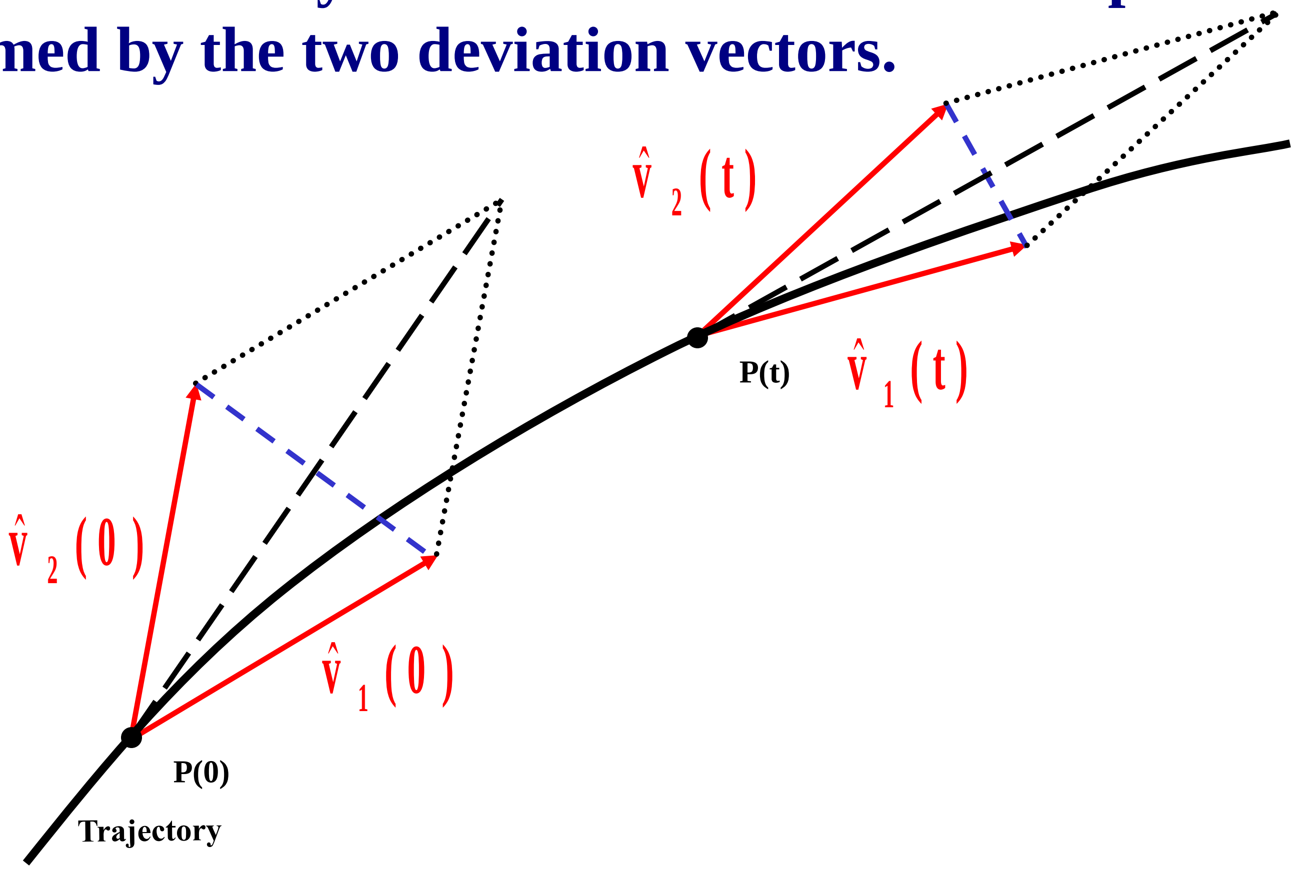

Definition of the Generalized Alignment Index (GALI)

SALI effectively measures the 'area' of the parallelogram formed by the two deviation vectors.

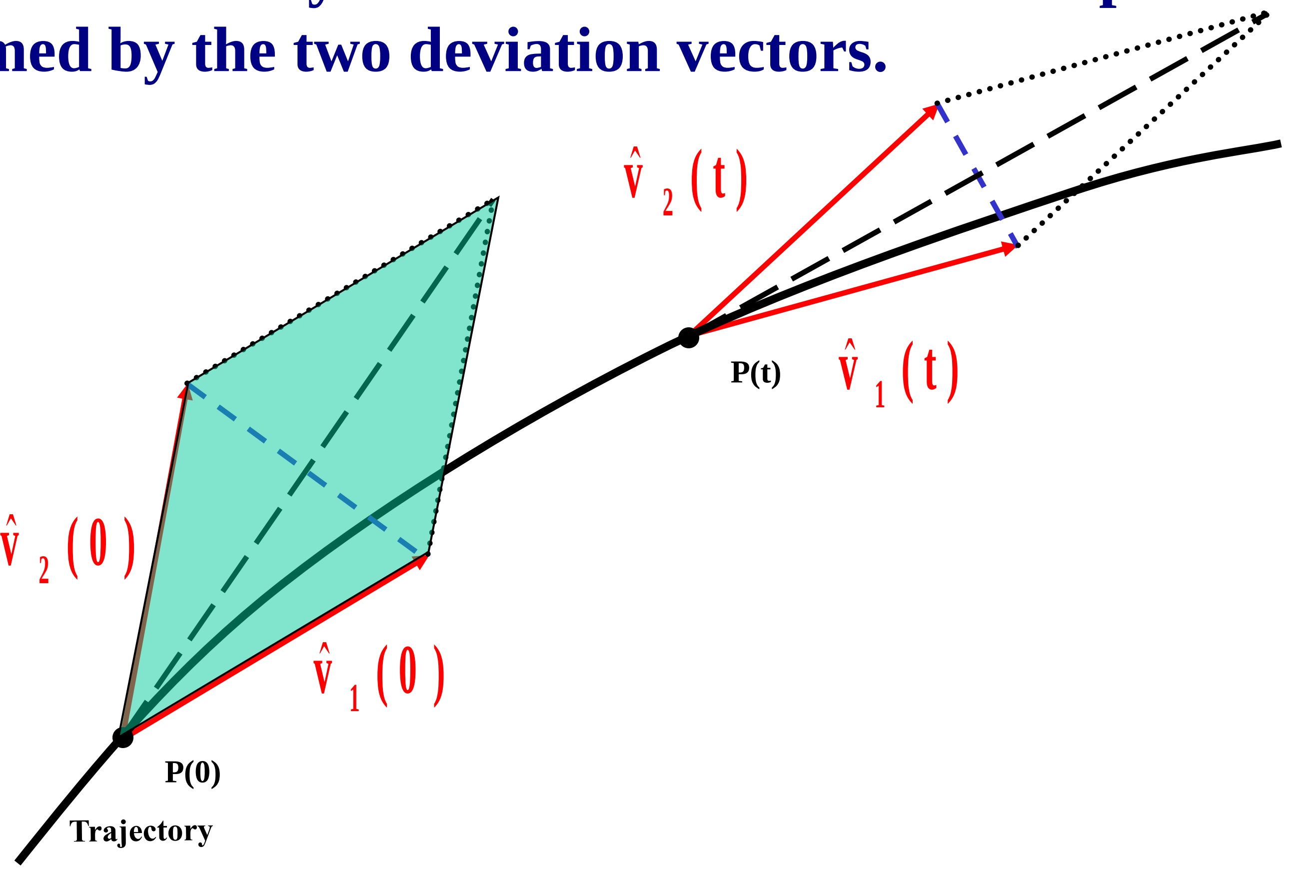

Definition of the Generalized Alignment Index (GALI)

SALI effectively measures the 'area' of the parallelogram formed by the two deviation vectors.

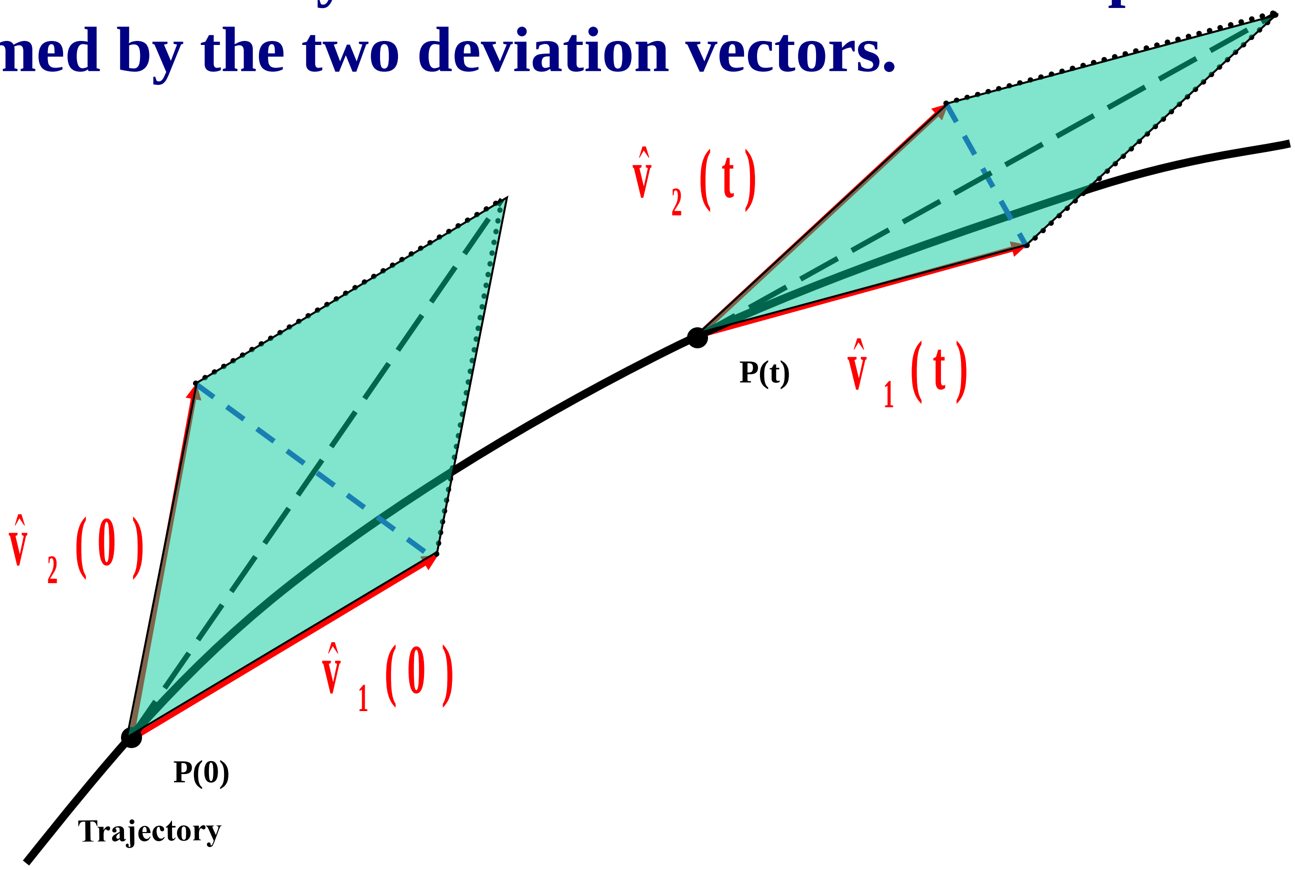

Definition of the Generalized Alignment Index (GALI)

SALI effectively measures the ‘area’ of the parallelogram formed by the two deviation vectors.

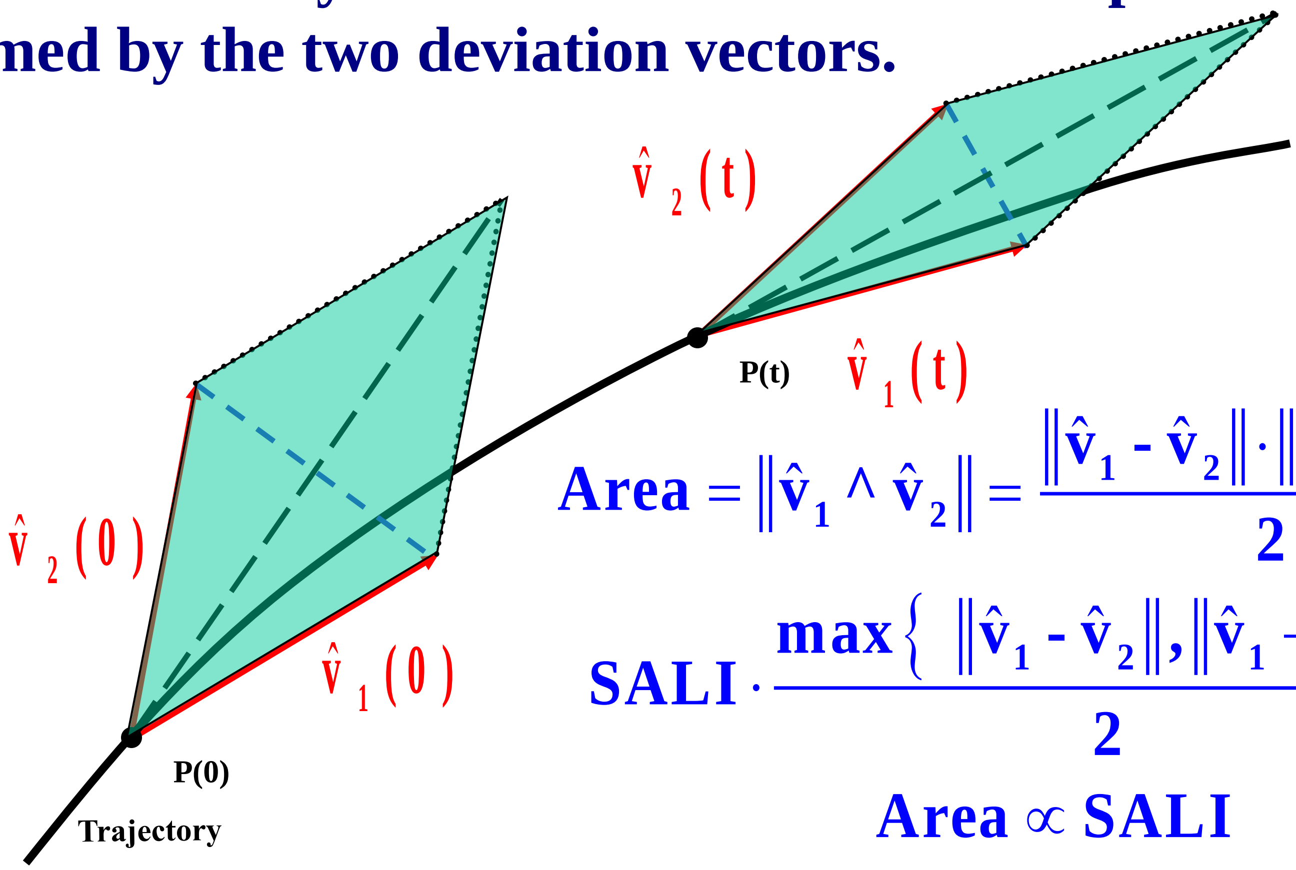

$$\mathbf{Area} = \|\hat{\mathbf{v}}_1 \wedge \hat{\mathbf{v}}_2\| = \frac{\|\hat{\mathbf{v}}_1 - \hat{\mathbf{v}}_2\| \cdot \|\hat{\mathbf{v}}_1 + \hat{\mathbf{v}}_2\|}{2} =$$

$$\mathbf{SALI} \cdot \frac{\max\left\{ \|\hat{\mathbf{v}}_1 - \hat{\mathbf{v}}_2\|, \|\hat{\mathbf{v}}_1 + \hat{\mathbf{v}}_2\| \right\}}{2} \Rightarrow$$

$$\mathbf{Area} \propto \mathbf{SALI}$$

Definition of the GALI

In the case of an N degree of freedom Hamiltonian system or a 2N symplectic map we follow the evolution of

k deviation vectors with $2 \leq k \leq 2N$,

and define (Ch.S., Bountis, Antonopoulos, 2007, Physica D) the Generalized Alignment Index (GALI) of order k :

$$GALI_k(t) = \left\| \hat{v}_1(t) \wedge \hat{v}_2(t) \wedge \ldots \wedge \hat{v}_k(t) \right\|$$

where

$$\hat{v}_1(t) = \frac{v_1(t)}{\left\| v_1(t) \right\|}$$

Behavior of the $GALI_k$ for chaotic motion

$GALI_k$ ($2 \leq k \leq 2N$) tends exponentially to zero with exponents that involve the values of the first k largest Lyapunov exponents $\sigma_1, \sigma_2, \ldots, \sigma_k$:

$$GALI_k(t) \propto e^{-[(\sigma_1-\sigma_2)+(\sigma_1-\sigma_3)+\ldots+(\sigma_1-\sigma_k)]t}$$

The above relation is valid even if some Lyapunov exponents are equal, or very close to each other.

Behavior of the $GALI_k$ for chaotic motion

N particles Fermi-Pasta-Ulam (FPU) system:

$$H = \frac{1}{2}\sum_{i=1}^{N} p_i^2 + \sum_{i=0}^{N}\left[\frac{1}{2}(q_{i+1} - q_i)^2 + \frac{\beta}{4}(q_{i+1} - q_i)^4\right]$$

with fixed boundary conditions, N=8 and β=1.5.

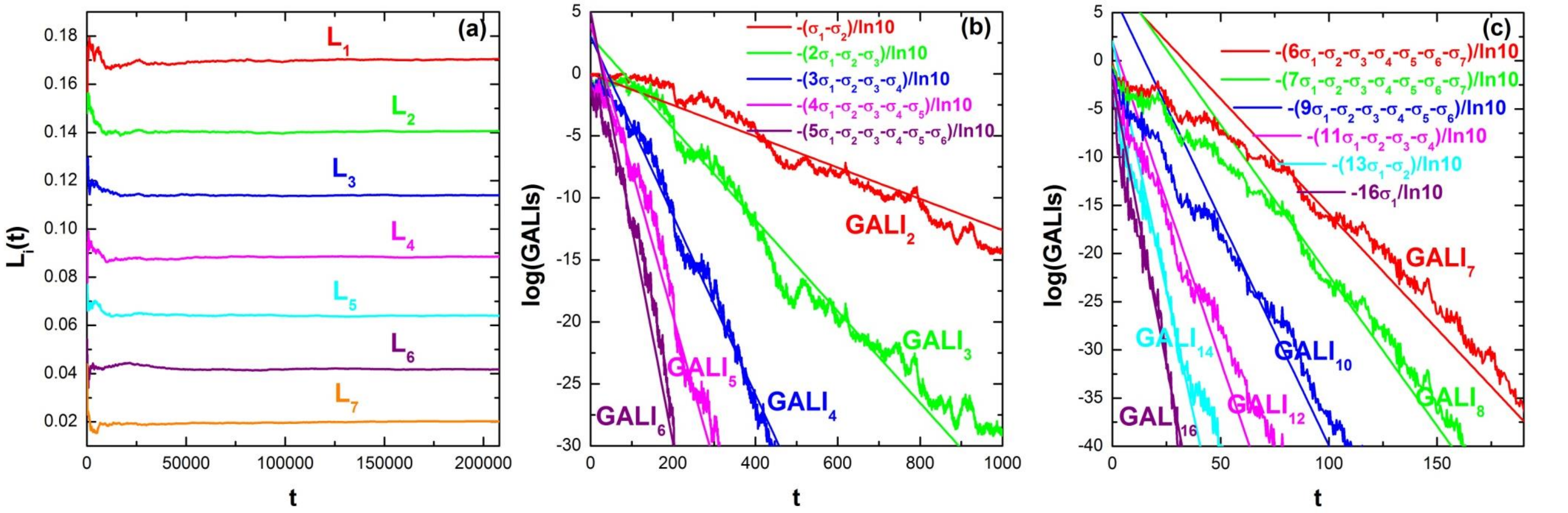

Behavior of the $GALI_k$ for regular motion

If the motion occurs on an s-dimensional torus with s≤N then the behavior of $GALI_k$ is given by (Ch.S., Bountis, Antonopoulos, 2008, Eur. Phys. J. Sp. Top.):

$$GALI_k(t) \propto \begin{cases} \text{constant} & \text{if} \quad 2 \le k \le s \\ \dfrac{1}{t^{k-s}} & \text{if} \quad s < k \le 2N - s \\ \dfrac{1}{t^{2(k-N)}} & \text{if} \quad 2N - s < k \le 2N \end{cases}$$

while in the common case with s=N we have :

$$GALI_k(t) \propto \begin{cases} \text{constant} & \text{if} \quad 2 \le k \le N \\ \dfrac{1}{t^{2(k-N)}} & \text{if} \quad N < k \le 2N \end{cases}$$

Behavior of the $GALI_k$ for regular motion

N=8 FPU system

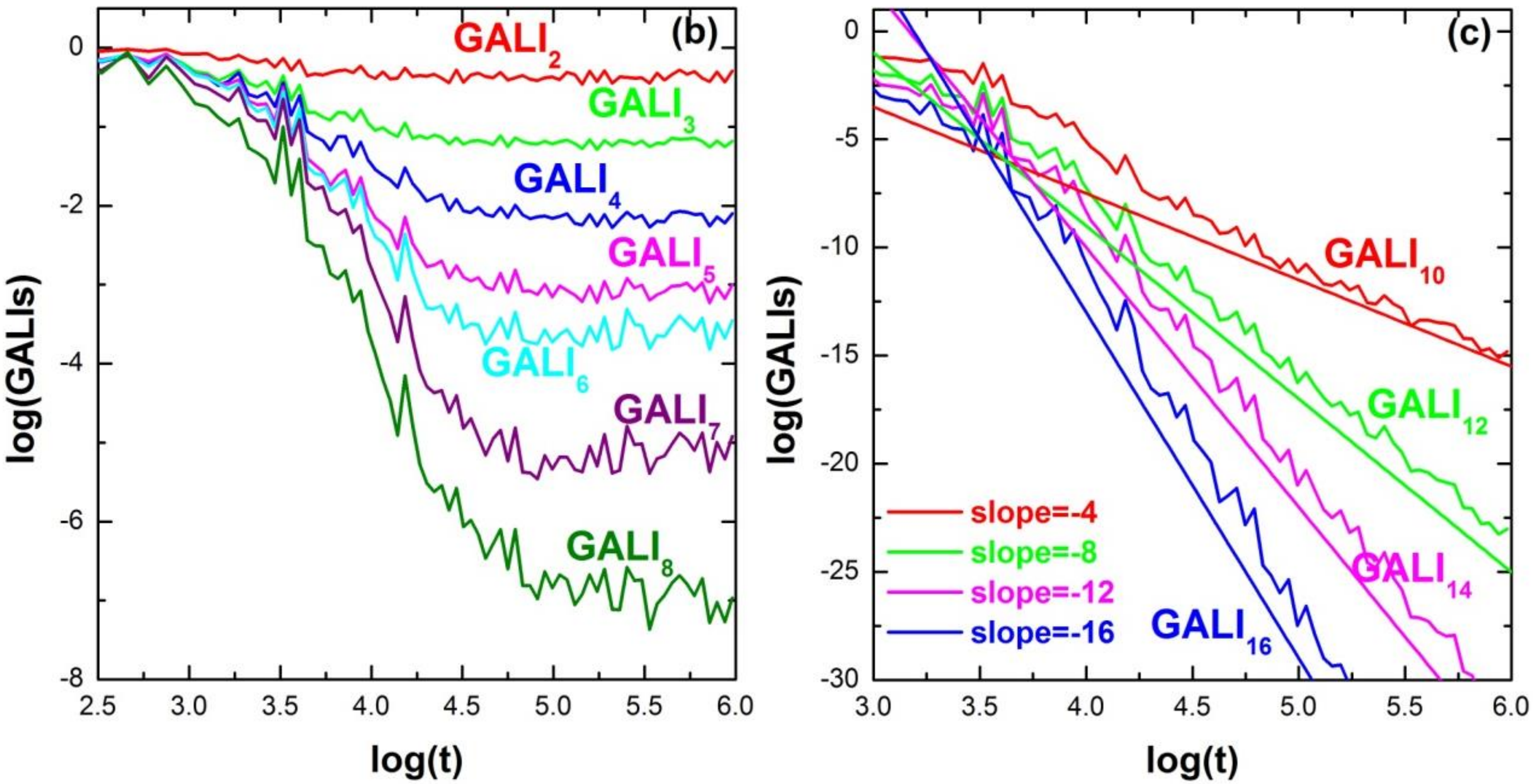

Global dynamics

- **GALI$_2$ (practically equivalent to the use of SALI)**
- **GALI$_N$**

Chaotic motion: GALI$_N$→0 (exponential decay)

Regular motion: GALI$_N$→constant≠0

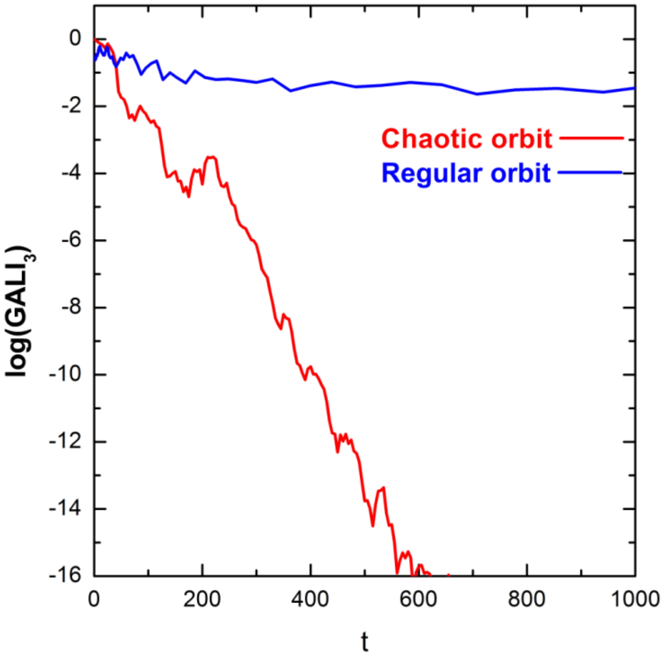

3D Hamiltonian

Subspace $q_3=p_3=0$, $p_2\geq0$ for t=1000.

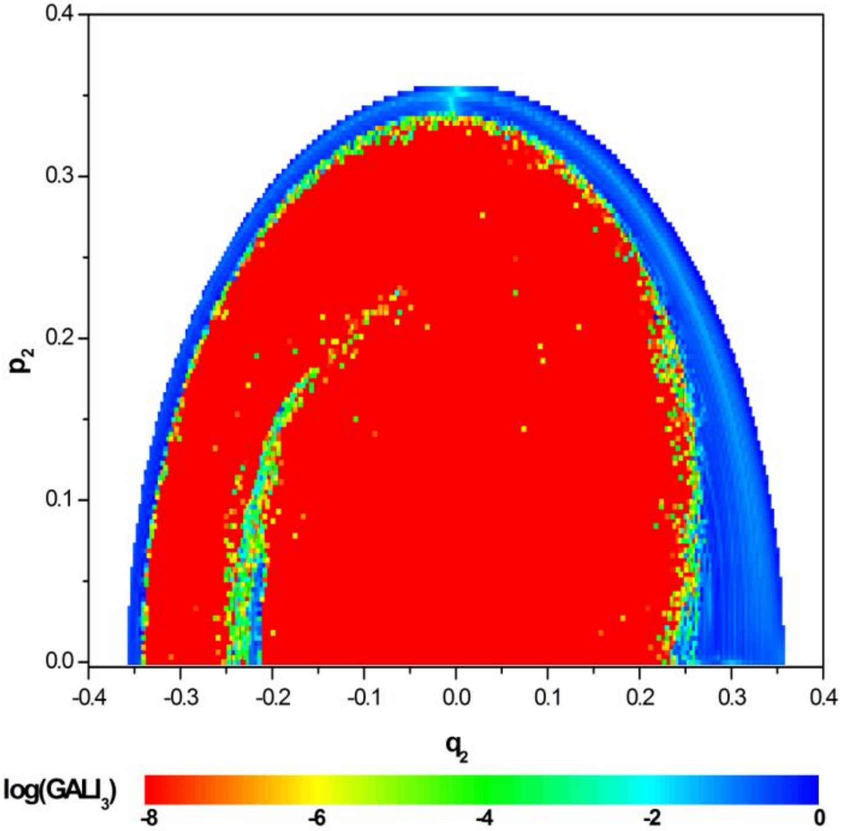

Global dynamics

GALI$_k$ with k>N

The index tends to zero both for regular and chaotic orbits but with completely different time rates:

Chaotic motion: exponential decay

Regular motion: power law

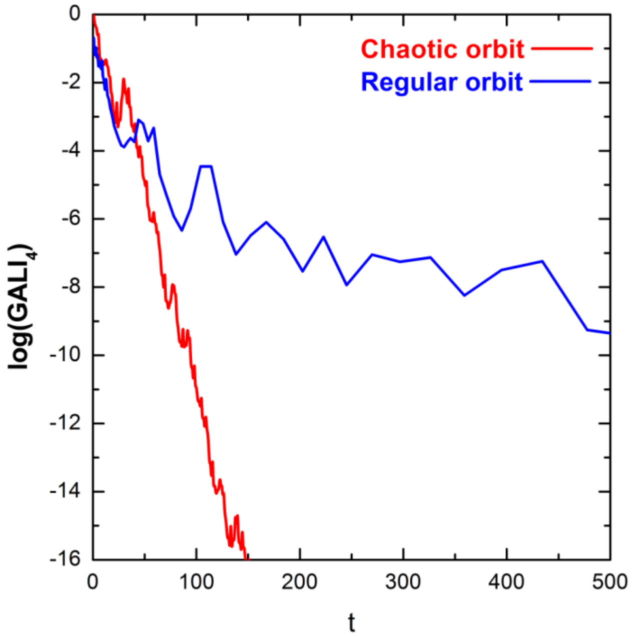

2D Hamiltonian (Hénon-Heiles)
Time needed for GALI$_4$<10^{-12}

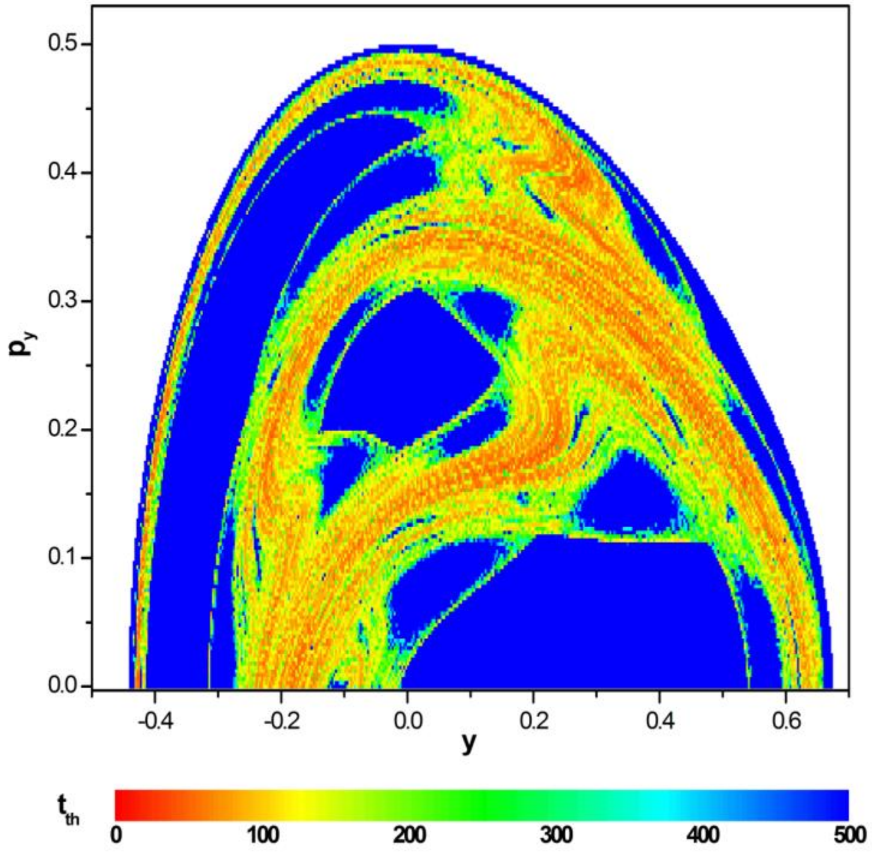

A time-dependent Hamiltonian system

Barred galaxies

NGC 1433

NGC 2217

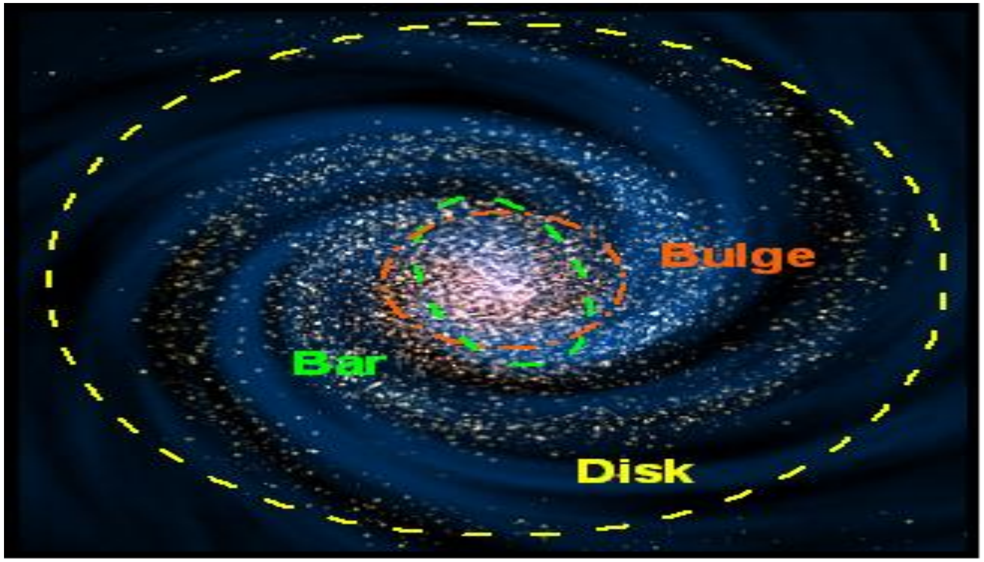

Barred galaxy model

The 3D bar rotates around its short *z*-axis (*x*: long axis and *y*: intermediate). The Hamiltonian that describes the motion for this model is:

$$H = \frac{1}{2}(p_x^2 + p_y^2 + p_z^2) + V(x,y,z) - \Omega_b(xp_y - yp_x) \equiv Energy$$

This model consists of the superposition of potentials describing an axisymmetric part and a bar component of the galaxy (Manos, Bountis, Ch.S., 2013, J. Phys. A).

a) Axisymmetric component:

i) Plummer sphere:

$$V_{sphere}(x,y,z) = -\frac{GM_S}{\sqrt{x^2+y^2+z^2+\varepsilon_s^{\,2}}}$$

ii) Miyamoto–Nagai disc:

$$V_{disc}(x,y,z) = -\frac{GM_D}{\sqrt{x^2+y^2+(A+\sqrt{B^2+z^2})^2}}$$

b) Bar component:

$$V_{bar}(x,y,z) = -\pi Gabc\,\frac{\rho_c}{n+1}\int_\lambda^\infty \frac{du}{\Delta(u)}(1-m^2(u))^{n+1},$$

(Ferrers bar)

$$\rho_c = \frac{105}{32\pi}\frac{GM_B}{abc}$$

$$where\ m^2(u) = \frac{x^2}{a^2+u} + \frac{y^2}{b^2+u} + \frac{z^2}{c^2+u},\quad \Delta^2(u) = (a^2+u)(b^2+u)(c^2+u),$$

n: positive integer ($n=2$ for our model), λ: the unique positive solution of $m^2(\lambda)=1$

Its density is:

$$\rho = \begin{cases} \rho_c(1-m^2)^n, & \text{for } m \le 1 \\ 0, & \text{for } m > 1 \end{cases},\quad \text{where } m^2 = \frac{x^2}{a^2} + \frac{y^2}{b^2} + \frac{z^2}{c^2},\ a > b > c \text{ and } n = 2.$$

Time-dependent barred galaxy model

The 3D bar rotates around its short *z*-axis (*x*: long axis and *y*: intermediate). The Hamiltonian that describes the motion for this model is:

$$H = \frac{1}{2}(p_x^2 + p_y^2 + p_z^2) + V(x,y,z,t) - \Omega_b(xp_y - yp_x) \equiv Energy$$

This model consists of the superposition of potentials describing an axisymmetric part and a bar component of the galaxy (Manos, Bountis, Ch.S., 2013, J. Phys. A).

a) Axisymmetric component:

$$M_S + M_B(t) + M_D(t) = 1, \quad \text{with} \quad M_B(t) = M_B(0) + \alpha t$$

i) Plummer sphere:

$$V_{sphere}(x,y,z) = -\frac{GM_S}{\sqrt{x^2 + y^2 + z^2 + \varepsilon_s^2}}$$

ii) Miyamoto–Nagai disc:

$$V_{disc}(x,y,z) = -\frac{GM_D(t)}{\sqrt{x^2 + y^2 + (A + \sqrt{B^2 + z^2})^2}}$$

b) Bar component:

$$V_{bar}(x,y,z) = -\pi Gabc \frac{\rho_c}{n+1} \int_\lambda^\infty \frac{du}{\Delta(u)} (1 - m^2(u))^{n+1},$$

(Ferrers bar)

$$\rho_c = \frac{105}{32\pi} \frac{GM_B(t)}{abc}$$

where $m^2(u) = \frac{x^2}{a^2+u} + \frac{y^2}{b^2+u} + \frac{z^2}{c^2+u}$, $\Delta^2(u) = (a^2+u)(b^2+u)(c^2+u)$,

n: positive integer ($n = 2$ for our model), λ: the unique positive solution of $m^2(\lambda) = 1$

Its density is:

$$\rho = \begin{cases} \rho_c (1 - m^2)^n, & \text{for } m \le 1 \\ 0, & \text{for } m > 1 \end{cases}, \quad \text{where } m^2 = \frac{x^2}{a^2} + \frac{y^2}{b^2} + \frac{z^2}{c^2}, \; a > b > c \text{ and } n = 2.$$

Time-dependent 2D barred galaxy model

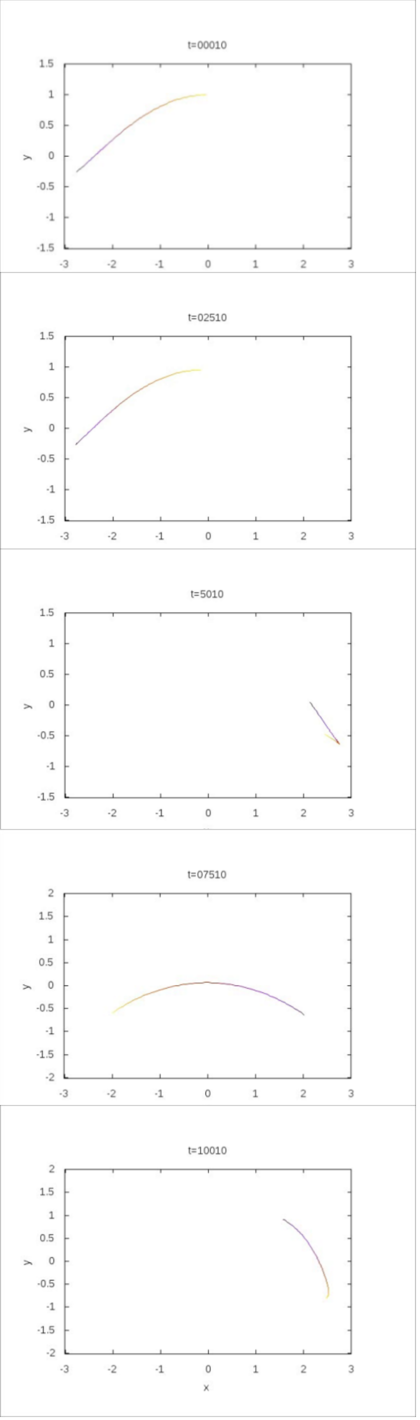

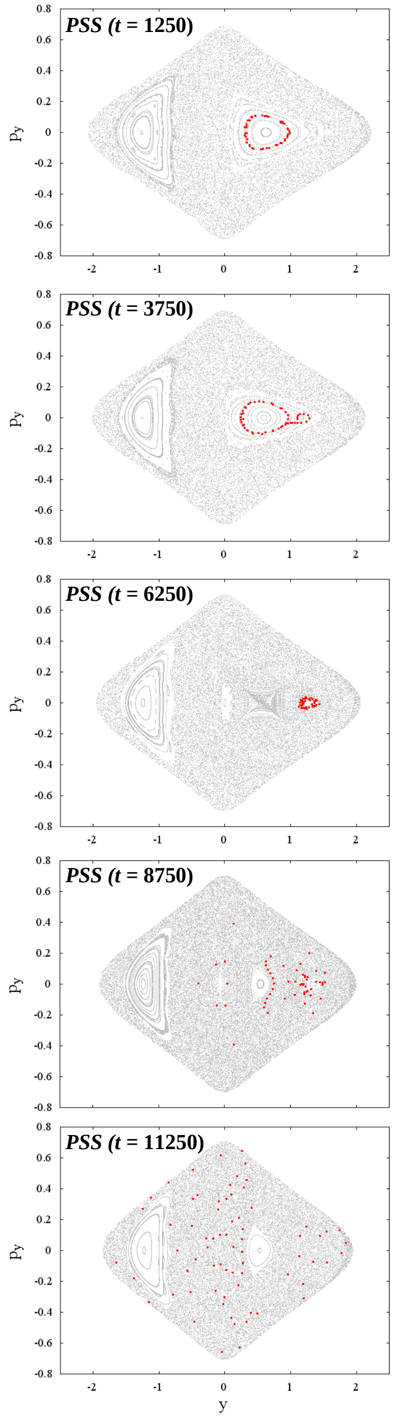

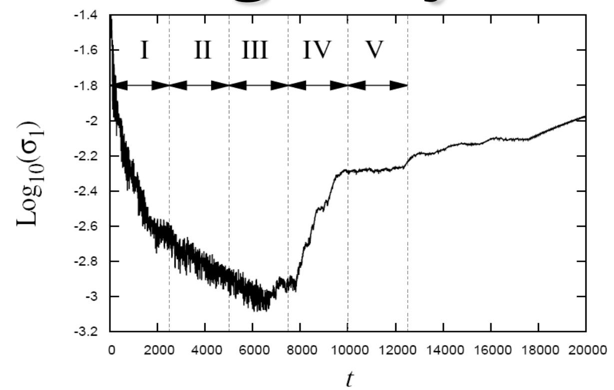

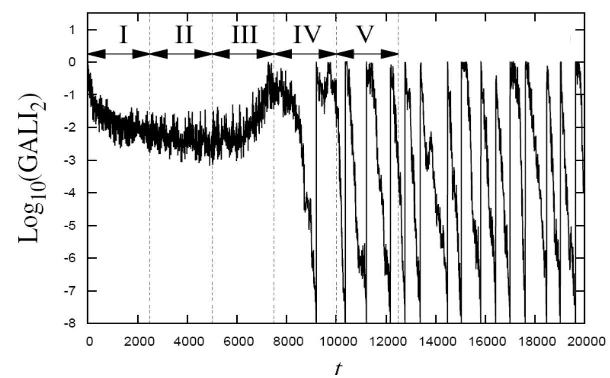

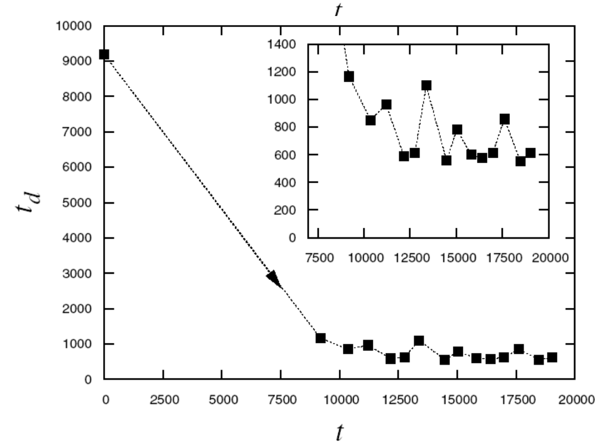

Time-dependent 3D barred galaxy model

Interplay between chaotic and regular motion

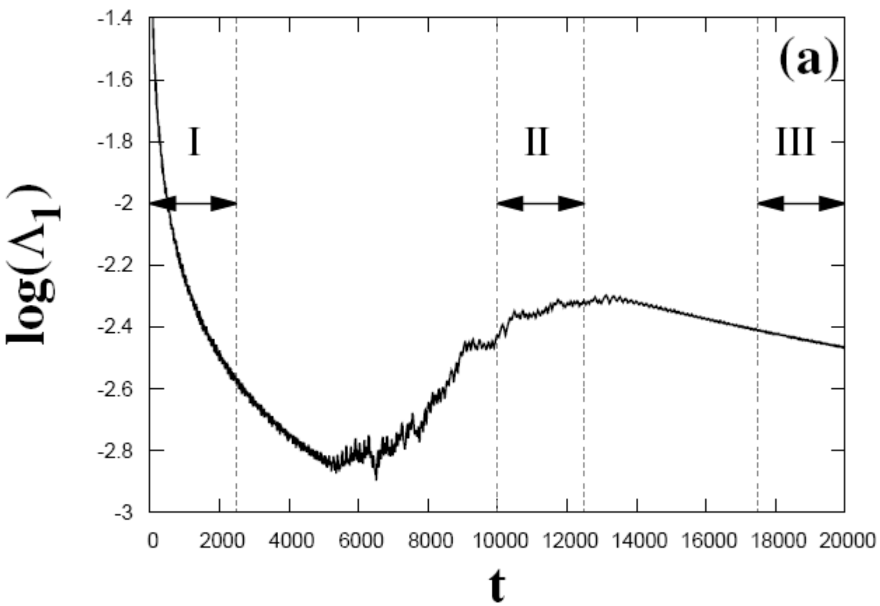

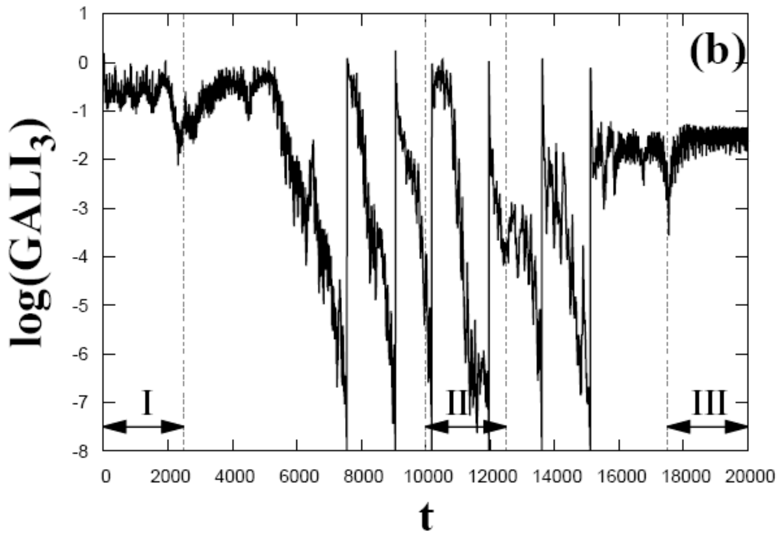

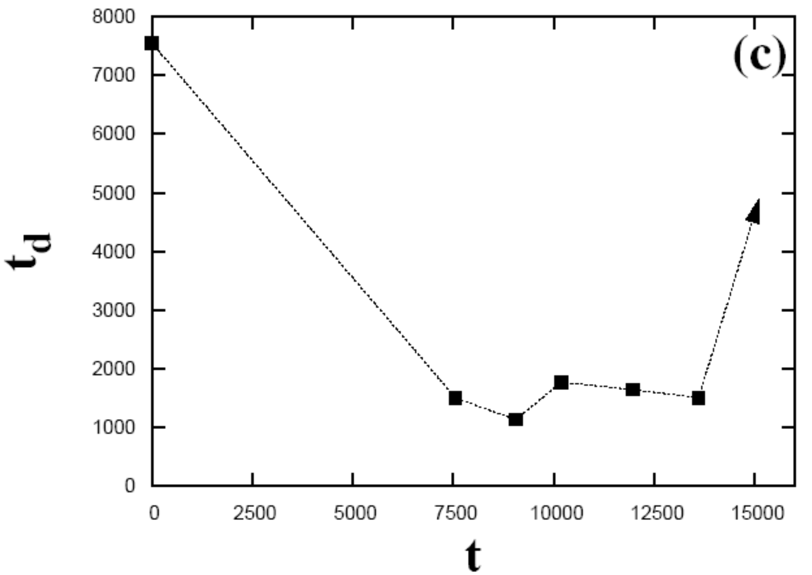

Summary

- **The Smaller (SALI) and the Generalized (GALI) ALignment Index methods are fast, efficient and easy to compute chaos indicator.**

- **Behaviour of the Generalized ALignment Index of order k ($GALI_k$):**
  - ✓ **Chaotic motion: it tends exponentially to zero**
  - ✓ **Regular motion: it fluctuates around non-zero values (or goes to zero following power-laws)**

- **$GALI_k$ indices :**
  - ✓ **can distinguish rapidly and with certainty between regular and chaotic motion**
  - ✓ **can be used to characterize individual orbits as well as "chart" chaotic and regular domains in phase space**
  - ✓ **can identify regular motion on low–dimensional tori**
  - ✓ **are perfectly suited for studying the global dynamics of multidimentonal systems, as well as <u>of time-dependent models</u>**

Main References

- Lyapunov exponents
  - ✓ Ch.S. (2010) Lect. Notes Phys., 790, 63

- Reviews on SALI and GALI
  - ✓ Bountis T C & Ch.S. (2012) ‘Complex Hamiltonian Dynamics’, Chapter 5, Springer Series in Synergetics
  - ✓ Ch.S. & Manos T (2016) Lect. Notes Phys., 915, 129

- SALI
  - ✓ Ch.S. (2001) J. Phys. A, 34, 10029
  - ✓ Ch.S., Antonopoulos Ch, Bountis T C & Vrahatis M N (2003) Prog. Theor. Phys. Supp., 150, 439
  - ✓ Ch.S., Antonopoulos Ch, Bountis T C & Vrahatis M N (2004) J. Phys. A, 37, 6269
  - ✓ Bountis T & Ch.S. (2006) Nucl. Inst Meth. Phys Res. A, 561, 173
  - ✓ Boreaux J, Carletti T, Ch.S. &Vittot M (2012) Com. Nonlin. Sci. Num. Sim., 17, 1725
  - ✓ Boreaux J, Carletti T, Ch.S., Papaphilippou Y & Vittot M (2012) Int. J. Bif. Chaos, 22, 1250219

- GALI
  - ✓ Ch.S., Bountis T C & Antonopoulos Ch (2007) Physica D, 231, 30
  - ✓ Ch.S., Bountis T C & Antonopoulos Ch (2008) Eur. Phys. J. Sp. Top., 165, 5
  - ✓ Gerlach E, Eggl S & Ch.S. (2012) Int. J. Bif. Chaos, 22, 1250216
  - ✓ Manos T, Ch.S. & Antonopoulos Ch (2012) Int. J. Bif. Chaos, 22, 1250218
  - ✓ Manos T, Bountis T & Ch.S. (2013) J. Phys. A, 46, 254017
  - ✓ Moges H, Manos T & Ch.S. (2020) Nonlin. Phenom. Complex Syst., 23, 153

A …shameless promotion

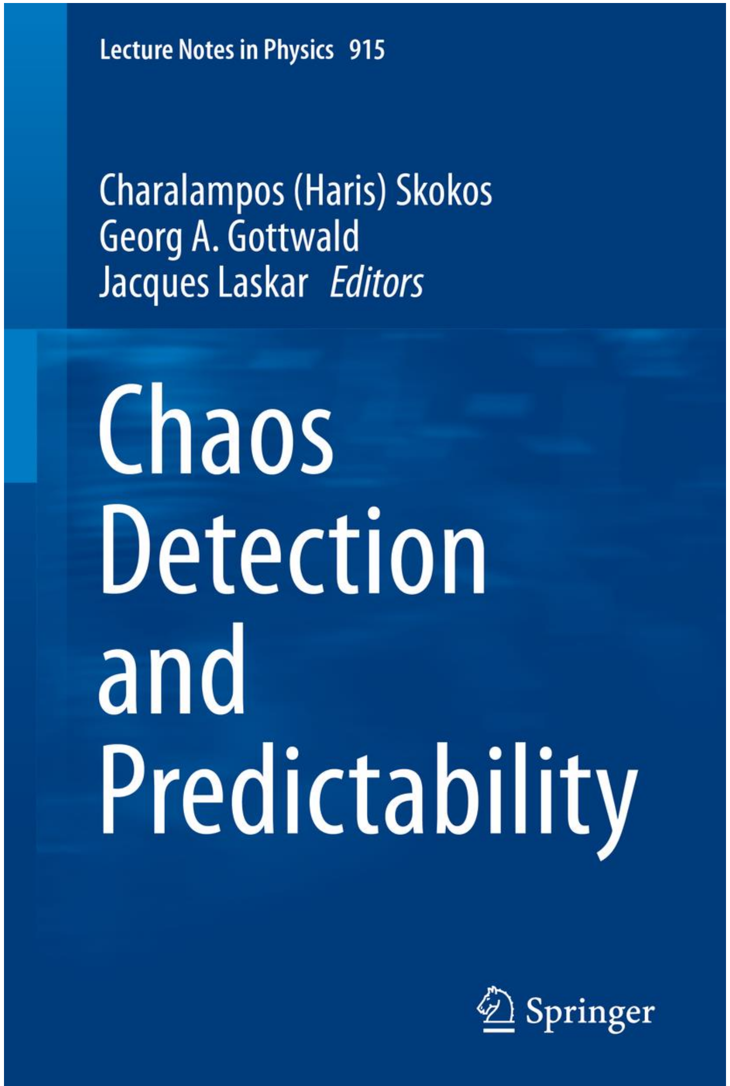

2016, Lect. Notes Phys., 915, Springer

Contents